

The Role of Echocardiography During Mitral Valve Percutaneous Interventions

Nina C. Wunderlich, MD^{a,b}, Roy Beigel, MD^{c,d,e},
Robert J. Siegel, MD^{c,*}

KEYWORDS

- Echocardiography • Mitral stenosis • Mitral regurgitation • Paravalvular leak
- Percutaneous intervention

KEY POINTS

- As the mitral leaflets cannot be assessed by fluoroscopy, preprocedural assessment, procedural guidance, and postprocedural assessment of percutaneous mitral interventions for mitral valve stenosis (MS), mitral regurgitation (MR), and mitral valve (MV) paravalvular leaks (PVLs) rely heavily on echocardiography.
- Although two-dimensional (2D) transesophageal echocardiography (TEE) has played a major role in guidance of the procedures, three-dimensional (3D) TEE provides more detailed information on MV anatomy and catheter and device positions.
- Combining 2D and 3D TEE improves results and reduces procedure time.

INTRODUCTION

TEE is routinely used to guide percutaneous interventions involving the MV. The most common percutaneous procedures are (1) percutaneous mitral balloon valvuloplasty (PMBV) for rheumatic MS, (2) edge-to-edge repair with the MitraClip (Abbott Laboratories, Abbott Park, IL, USA) for MR, and (3) closure of prosthetic paravalvular mitral leakages (PVML). 3D TEE has become an important adjunct in patient selection and is, in some cases, critical for intraprocedural guidance for percutaneous mitral interventions.

PERCUTANEOUS MITRAL BALLOON VALVULOPLASTY

PMBV, a safe and effective treatment of MS,^{1–9} is the preferred treatment option for selected

symptomatic patients with MS.^{10–12} Rheumatic fever, the leading cause of MS,^{13,14} causes commissural fusion of the valve, narrowing of the valve orifice, and valve obstruction. Commissural fusion (**Fig. 1A, B**) is the requisite lesion for PMBV to be effective. PMBV is not effective for degenerative calcific MS, where heavy mitral annular calcification is the main lesion.

Preprocedural Assessment of MS Severity

Evaluation of MS includes assessment of the valve area, the mean Doppler gradients, and pulmonary artery pressure (**Table 1**).^{10,11,15} 2D planimetry of the mitral valve area (MVA) is performed from the parasternal short axis view when the maximal diastolic orifice is present (see **Fig. 1B**). The entire MV orifice should be seen. High gain settings should be avoided, as they may lead to underestimation

Conflict of Interest: None.

^a Cardiovascular Center, Darmstadt, Germany; ^b University Hospital, Mainz, Germany; ^c The Heart Institute, Cedars Sinai Medical Center, 8700 Beverly Blvd, Los Angeles, CA 90048, USA; ^d The Leviev Heart Center, Sheba Medical Center, Tel-Hashomer 52621, Israel; ^e Sackler School of Medicine, Tel Aviv University, Tel Aviv, Israel

* Corresponding author.

E-mail address: siegel@cshs.org

Cardiol Clin 31 (2013) 237–270

<http://dx.doi.org/10.1016/j.ccl.2013.03.003>

0733-8651/13/\$ – see front matter © 2013 Elsevier Inc. All rights reserved.

Downloaded for Anonymous User (n/a) at Brazilian Society of Cardiology from ClinicalKey.com by Elsevier on May 19, 2021. For personal use only. No other uses without permission. Copyright ©2021. Elsevier Inc. All rights reserved.

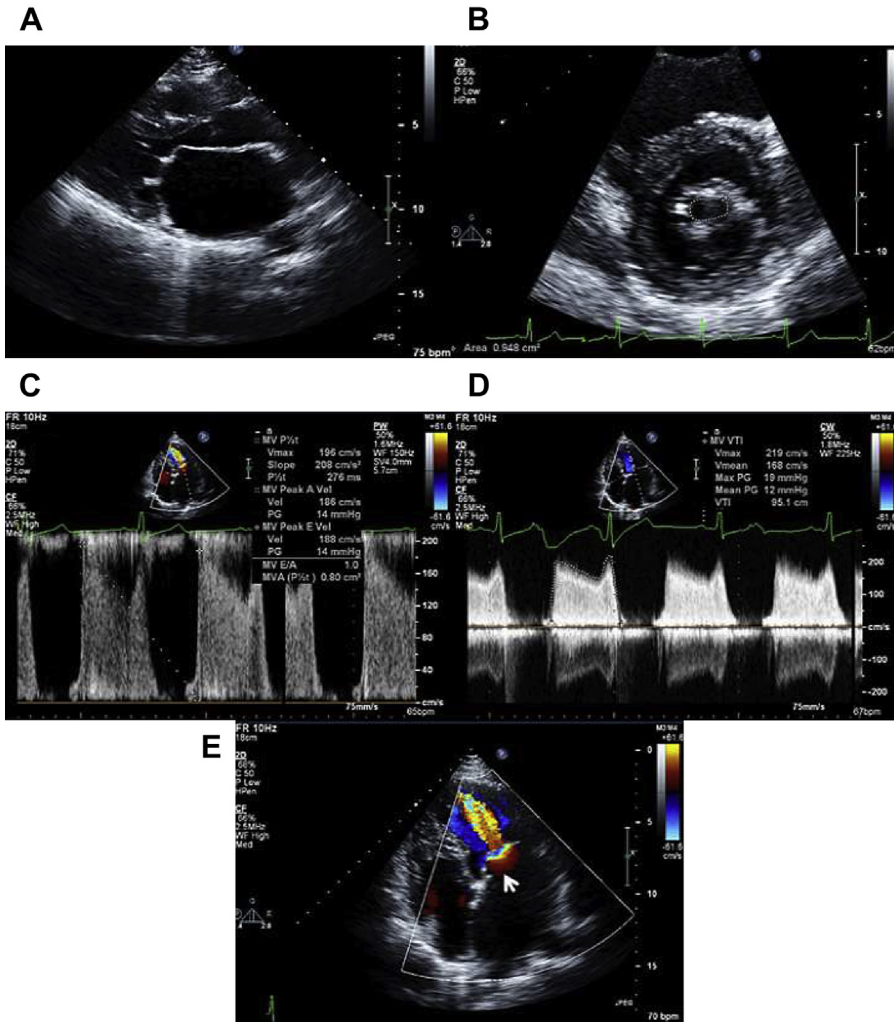


Fig. 1. Transthoracic 2D parasternal long axis view (A) demonstrating commissural fusion with a restricted mitral valve. In the short axis view (B), 2D planimetry of the mitral valve area is performed in the parasternal short axis view at the tip of the leaflets when maximal excursion of the leaflets is seen. The inner edge of the MV orifice is traced in the midsystole. Doppler echocardiography using the pressure half-time ($T_{1/2}$) method (C). $T_{1/2}$ is obtained by tracing the deceleration slope of the E-wave on Doppler spectral display of transmitral inflow, and in the case shown it is 279 ms, resulting in an estimated valve area of $220/279 = 0.8 \text{ cm}^2$. The MV area can be calculated from the following formula: $220/(T_{1/2})$. (D) Doppler measurements using the continuous wave Doppler signal across the mitral valve showing a mean pressure gradient of 12 mm Hg consistent with severe mitral stenosis. (E) The continuity equation and proximal isovelocity surface area (PISA; white arrow) methods can also be used for quantification of MS severity.

of MVA. Planimetry correlates with the anatomic valve area as assessed on explanted valves.¹⁶ Some reports indicate planimetry by 3D echo is more accurate and reproducible than 2D echocardiography.^{17–19}

Mitral maximal and mean Doppler gradients are also calculated. The maximal gradient, derived from peak mitral velocity, is influenced by left atrial (LA) compliance and left ventricular (LV) diastolic function.²⁰ However, the mean MV gradient more

accurately reflects MS severity. Continuous wave (CW) Doppler measurements across the MV have good correlation with invasive measurements using transeptal (TS) catheterization (see Fig. 1D).²¹ Mitral transvalvular gradients are highly rate and flow dependent, as the transmitral gradient is a function of the square of the transvalvular flow. Thus, heart rate and cardiac output significantly affect the transmitral diastolic gradient (see Table 1, Appendix A—MS assessment).²²

Table 1
Methods and quantification of mitral valve stenosis severity

	Quantification of Severity	Method	Limitations
Valve area (cm²)			
Pressure half-time ($T_{1/2}$) (see Fig. 1C, Appendix A)	Mild >1.5 Moderate 1–1.5 Severe <1	$220/(T_{1/2})$	Aortic regurgitation Atrial septal defects Previous surgical/percutaneous mitral valvuloplasty
Planimetry (see Fig. 1B) Continuity equation (Appendix A)		Tracing the inner edge of the MV orifice in midsystole $\pi \left(\frac{D2}{4} \right) \left(\frac{VTI \text{ aorta (cm)}}{VTI \text{ mitral (cm)}} \right)$	Underestimation due to high gain Limited accuracy and reproducibility Atrial fibrillation Aortic and/or mitral regurgitation
Proximal isovelocity (PISA) (Appendix A)		$\pi (r^2)(V_{alias})/Peak V_{mitral} \times \alpha/180^\circ$	Technically demanding
Mean gradient (mm Hg) (see Fig. 1D)	Mild <5 Moderate 5–10 Severe >10	Tracing of the Doppler diastolic mitral flow profile	Heart rate and flow dependent
Pulmonary artery systolic pressure (mm Hg)	Mild <30 Moderate 30–50 Severe >50	Tricuspid regurgitation gradient + right atrial pressure	Underestimation due to malalignment Inaccurate estimation of right atrial pressure

Assessment of Valve Anatomy and Suitability for PMBV

Echocardiographic evaluation of the mitral valve anatomy and pathology dictates the feasibility and likelihood of successful PMBV (Figs. 2 and 3, Table 2).

- The Wilkins score (see Table 2)²³ is most commonly used for transthoracic echocardiographic (TTE) assessment: 2D echo is used to evaluate valve morphologic leaflet mobility, flexibility, thickness, calcification, subvalvular fusion, commissural fusion, and calcification. The features that determine suitability for PMBV have been used to develop different scoring systems.^{1,23–27} Each feature is graded on a 1 to 4 scale yielding a maximum score of 16. A score greater than 8 suggests the valve may not be suitable for PMBV.
- Assessment of commissural calcium²⁷ (see Figs. 2 and 3): The extent of commissural calcification is quantified by giving each half commissure (anterolateral and posteromedial) with detection of high-intensity bright echos a score of 1. Commissural calcification can, therefore, range from grade 0 to grade 4 (see Fig. 3). The grade of intercommissural calcium is a significant predictor of achieving

an MVA post-PMVB²⁸ greater than 1.5 cm² without creating significant MR.²⁹ The usefulness is greatest in patients with a Wilkins score of 8 or less (= patients with relatively “good” valves), whereas in patients with a score greater than 8, calcium scoring does not add additional predictive value. Patients with commissural calcification grade 0/1 had larger valve areas and better improvement of symptoms than patients with grade 2/3.

- Echocardiographic grouping (Table 3)¹

The echocardiographic grouping is based on the echocardiographic and fluoroscopic (calcification) assessment of the following characteristics: valve mobility, fusion of the subvalvular apparatus, and the amount of leaflet calcification (see Table 3).

In a subset of 40 patients, a Wilkins score of 7 to 9 correlated with the echocardiographic group 1, range 8 to 12 correlated with group 2, and range 10 to 15 with group 3.³⁰

- Real-time 3D transthoracic echocardiographic (RT-TT3DE) score (Table 4)³¹: this score evaluates both mitral leaflets and the subvalvular apparatus. The RT-TT3DE score seems to be highly reproducible with good interobserver and intraobserver agreement

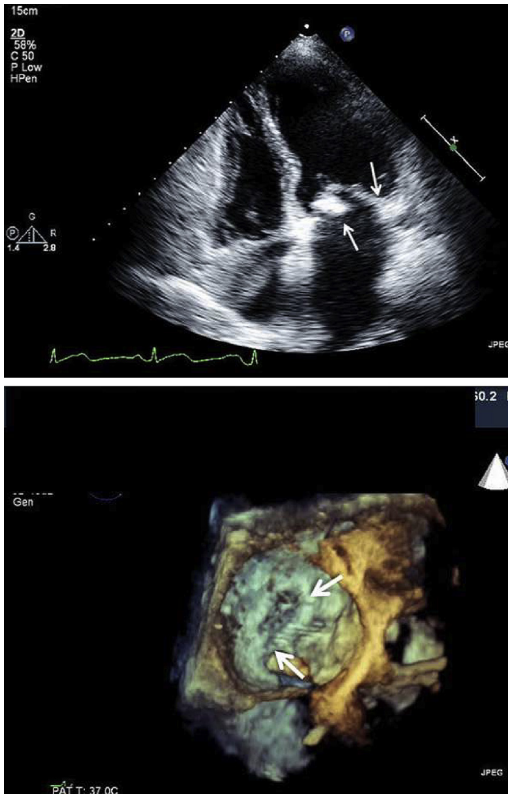


Fig. 2. Transthoracic 2D apical 4-chamber view (*top*) and 3D TEE reconstruction (*bottom*) showing severe commissural calcification (*arrows*), which makes the patient high risk for percutaneous balloon valvuloplasty.

in the assessment of MV morphology in patients with MS. RT-TT3DE is reported to be superior for detection of calcification and commissural splitting. Predictors of optimal PMBV were leaflet mobility and the involvement of the subvalvular apparatus. The incidence and severity of postprocedural MR was associated with a high calcification RT-TT3DE score.

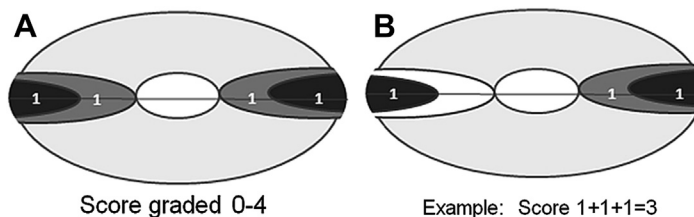


Fig. 3. Schematic of the evaluation of commissural calcification score. Commissural calcification is quantified by giving half commissure each (anterolateral and posteromedial) with detection of high-intensity bright echos a score of 1. Commissural calcification can therefore range from grade 0 (no calcification) to grade 4 (A) (both commissures are completely calcified). (B) gives an example where half a commissure is calcified on the left side and the entire commissure is calcified on the right side. The added score is therefore 3.

No scoring system has been proved to be superior; thus, they should be used in conjunction with one another as part of a comprehensive echocardiographic assessment of the valve pathology.

Intraprocedural Guidance

Different types of balloons are available (single balloon, double balloon, and Inoue balloon [Toray Medical Co, Ltd, Chiba, Japan]) for PMBV. The Inoue balloon, the most commonly used, had low intraprocedural and periprocedural mortality and a success rate of 95% or more. On average, MVA increases to 1.9 to 2.0 cm², and New York Heart Association (NYHA) functional improves to class I-II in 90% of the cases.⁸

When anticoagulation therapy is withheld before PMBV, thrombi can develop rapidly in patients with MS. Thus, before TS puncture, TEE should be done to exclude an LA thrombus and to reassess contraindications for PMBV (**Box 1**). Most interventionalists exclude patients with an LA thrombus (**Fig. 4**) for PMBV. If a thrombus is detected, the authors postpone the procedure until it has resolved on repeat TEE. Cases with excessive and/or nonresolving LA thrombus should be considered for surgery rather than for PMBV.^{10,11}

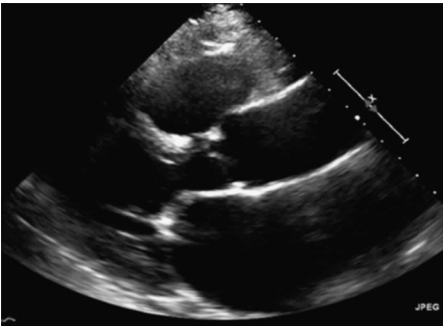
For most PMBV cases, the preferred TS puncture site is in the posterior, a more inferior region of the fossa ovalis. TEE or alternatively intracardiac echo guidance is helpful, especially in patients with dilated atria or unusual morphology of the interatrial septum (IAS) such as a large atrial septal aneurysm, prior IAS surgery, or distortion of the IAS from scoliosis or prior pneumectomy. The tip of the needle for TS puncture can be identified by a tentlike indentation of the IAS on TEE (**Fig. 5**). The height above the valve is best appreciated in the 4-chamber view (~0°), the anterior-posterior orientation is obtained using a short axis view at the base (30°–45°), and the superior-inferior orientation is seen on a long axis view (90°–100°). X-plane imaging facilitates the TS

Table 2
Echocardiographic scoring of the mitral valve (adapted from the Wilkins score)

Imaging Modality Views

Mitral Valve Scoring

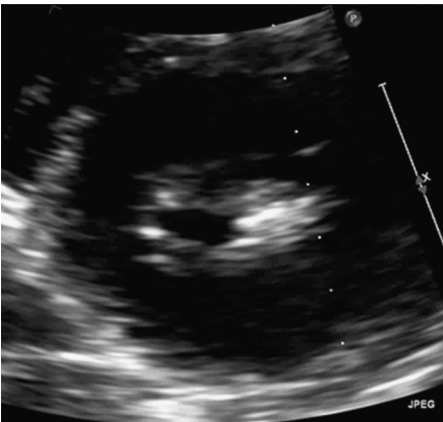
2D Parasternal long axis



The following characteristics are scored:
 Leaflet mobility

- 1 = Mobile valve, only leaflet tips restriction
- 2 = Leaflet mid and base portions with normal mobility
- 3 = Valve continues to move forward in diastole, mainly from the base
- 4 = Immobile or minimal mobile valve in diastole

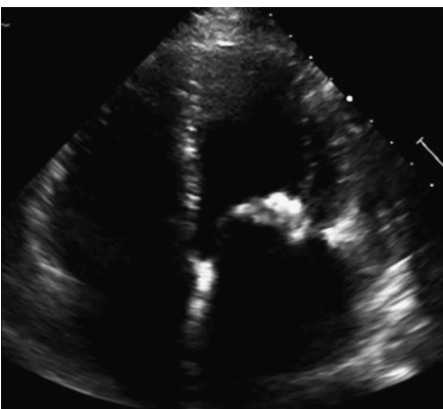
Parasternal short axis



Leaflet thickening

- 1 = Leaflet thickness 4–5 mm
- 2 = Mid leaflets normal, thickening of margins 5–8 mm
- 3 = Entire leaflet thickening 5–8 mm
- 4 = Thickening of all leaflet tissue >8–10 mm

Apical 4-chamber

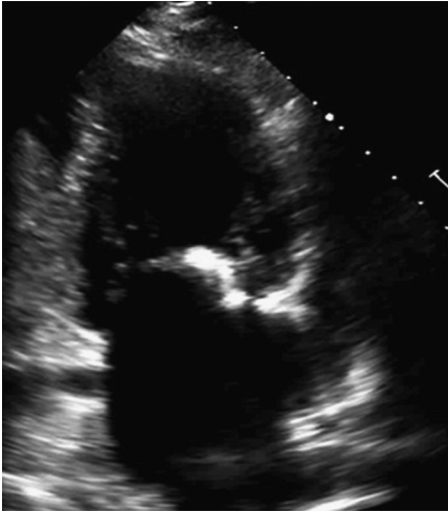


Leaflet calcification

- 1 = Single area of increased echo brightness
- 2 = Scattered areas of brightness confined to leaflet margins
- 3 = Brightness extending into midportions of the leaflets
- 4 = Extensive brightness throughout much of the tissue

(continued on next page)

Table 2
(continued)

Imaging Modality Views	Mitral Valve Scoring
Apical 2-chamber 	<p>Subvalvular involvement</p> <p>1 = Minimal thickening just below the MV leaflets</p> <p>2 = Thickening up to 1/3 of chordal length</p> <p>3 = Thickening extending to distal 1/3 of the chords</p> <p>4 = Extensive thickening of all chordal structures</p> <p>Maximal score: 16. A score >8 suggests the valve may not be suitable to percutaneous mitral balloon valvuloplasty</p>

puncture by showing simultaneous anterior-posterior and superior-inferior orientations.

After TS puncture, the PMBV catheter and the balloon are placed across the mitral valve leaflets

(Fig. 6). 2D and 3D TEE are useful in guiding delivery of catheters and wires across the MV, positioning the balloon within the mitral valve orifice, and confirming that the balloon is optimally positioned between the mitral leaflets. Inflation of the balloon in the subvalvular region should be avoided, as this may lead to valvular, chordal, or papillary muscle rupture (Fig. 7). As shown in Fig. 8, during balloon inflation, the mitral valve orifice is completely occluded, stasis is evident by echo, and hemodynamic deterioration may occur. Close monitoring of hemodynamic parameters is mandatory during this phase of the procedure. Dilatation of the MV orifice due to splitting of the commissures is evident by echo and fluoroscopy—the constriction of the balloon, visible at its waist at the level of the mitral leaflets, suddenly disappears.

Subsequently, echocardiographic reassessment is done for the following:

- Severity and location of MR (newly developed MR emerging from the commissures indicate a rupture of the valve leaflets) (1.4%–9.4% develop significant MR^{32,33})
- Mitral valve leaflet mobility
- Post-PMBV MVA using mean Doppler gradients, 2D and 3D MV planimetry (Fig. 9)
- Commissural opening (see Fig. 9D, E)

Table 3
Description of the 3 group grading of mitral valve anatomy as assessed by 2D echocardiography and fluoroscopy

Echocardiographic Group	Mitral Valve Anatomy
Group 1	Pliable, noncalcified anterior mitral leaflet and mild subvalvular disease, ie, thin chordate ≥ 10 mm long
Group 2	Pliable noncalcified anterior mitral leaflet and severe subvalvular disease, ie, thickened chordate < 10 mm long
Group 3	Calcification of MV of any extent, as assessed by fluoroscopy, whatever the state of the subvalvular apparatus

Table 4
Real-time transthoracic 3D echocardiographic score for the evaluation of mitral valve stenosis before percutaneous mitral balloon valvuloplasty

	Anterior Mitral Leaflet			Posterior Mitral Leaflet		
	A1	A2	A3	P1	P2	P3
Thickness (0–6) (0 = normal, 1 = thickened) ^a	0–1	0–1	0–1	0–1	0–1	0–1
Mobility (0–6) (0 = normal, 1 = thickened) ^a	0–1	0–1	0–1	0–1	0–1	0–1
Calcification (0–10) (0 = no, 1–2 = calcified) ^b	0–2	0–1	0–2	0–2	0–1	0–2
Subvalvular Apparatus^b						
	Proximal Third		Middle Third	Distal Third		
Thickness (0–3) (0 = normal, 1 = thickened)	0–1		0–1	0–1		
Separation (0–6) (0 = normal, 1 = partial, 2 = no)	0,1,2		0,1,2	0,1,2		

Each leaflet is divided into 3 segments (anterior leaflet: A1 [lateral], A2 [middle], A3 [medial]; posterior leaflet: P1 [lateral], P2 [middle], P3 [lateral]). Each segment is scored separately for thickness, mobility, and calcification. Normal thickness and mobility are scored as 0, whereas abnormal thickness or mobility is scored as 1. Absence of calcification is scored as 0, calcification in A2 or P2 (middle segments) is scored as 1, and calcification of commissural segments of both leaflets (A1, A3, and P1 and P3) is scored as 2. In addition, the anterior and posterior chordae are scored at a proximal (mitral valve level), a middle, and a distal (papillary muscle level) level. At each level, the anterior and the posterior leaflets are scored for thickness and separation in between. Normal thickness gets a score of 0, abnormal thickness a score of 1. Normal chordal separation (defined as distance in between >5 mm) is scored as 0, partial separation (defined as distance in between <5 mm) as 1, and absence of separation as 2. The individual score points are added up, the calculated total score ranges from 0 to 31 points. Mild mitral valve involvement was defined as <8 points, moderate MV involvement 8 to 13, and severe MV involvement ≥ 14 .

^a Normal = 0, mild = 1–2, moderate 3–4, severe ≥ 5 .

^b Normal = 0, mild = 1–2, moderate 3–5, severe ≥ 6 .

Adapted from Anwar AM, Attia WM, Nosir YF, et al. Validation of a new score for the assessment of mitral stenosis using real-time three-dimensional echocardiography. *J Am Soc Echocardiogr* 2010;23(1):13–22.

- Assessment of complications such as pericardial effusion and left-to-right shunt through the artificial atrial septal defect (ASD) secondary to the TS puncture.

The pressure half-time method (see **Fig. 1C**) post-PMBV is unreliable for calculation of MVA because of multiple factors: atrial compliance, a newly created ASD, and changes in hemodynamics influence this measurement.^{5,34–37}

Box 1
Contraindications to percutaneous mitral balloon valvuloplasty

- Mitral valve area greater than 1.5 cm²
- Left atrial thrombus
- More than mild mitral regurgitation
- Severe or bicommissural calcification
- Absence of commissural fusion
- Severe concomitant aortic valve disease or severe combined tricuspid stenosis and regurgitation
- Concomitant coronary artery disease requiring bypass surgery

RT 3D echocardiography is reported as having better accuracy and agreement with invasively determined MVA compared with conventional 2D planimetry³⁸ and superior in assessing commissural opening than 2D echo.

Successful PMBV has been defined as an MVA 1.5 cm² or more or 1.0 cm² or more, MR 2+ or less, and absence of complications.^{10,11} **Table 5** lists predictors of outcome after PMBV, which include a variety of clinical, morphologic, and hemodynamic parameters. **Box 2** summarizes the periinterventional role of echocardiography.

EDGE-TO-EDGE REPAIR WITH THE MITRACLIP FOR MITRAL REGURGITATION

Alfieri⁴⁵ developed a surgical technique of suturing the free edges of the mid portions of the anterior (A2) and posterior (P2) mitral valve scallops to create a double mitral valve orifice to treat MR. St. Goar developed the MitraClip as a catheter-based approach to create a double MV orifice and thereby reduce MR (St. Goar, personal communication, 2005).

The MitraClip system (**Fig. 10**) is the only percutaneous method available to alter the mitral valve morphology and annulus diameter and reduce

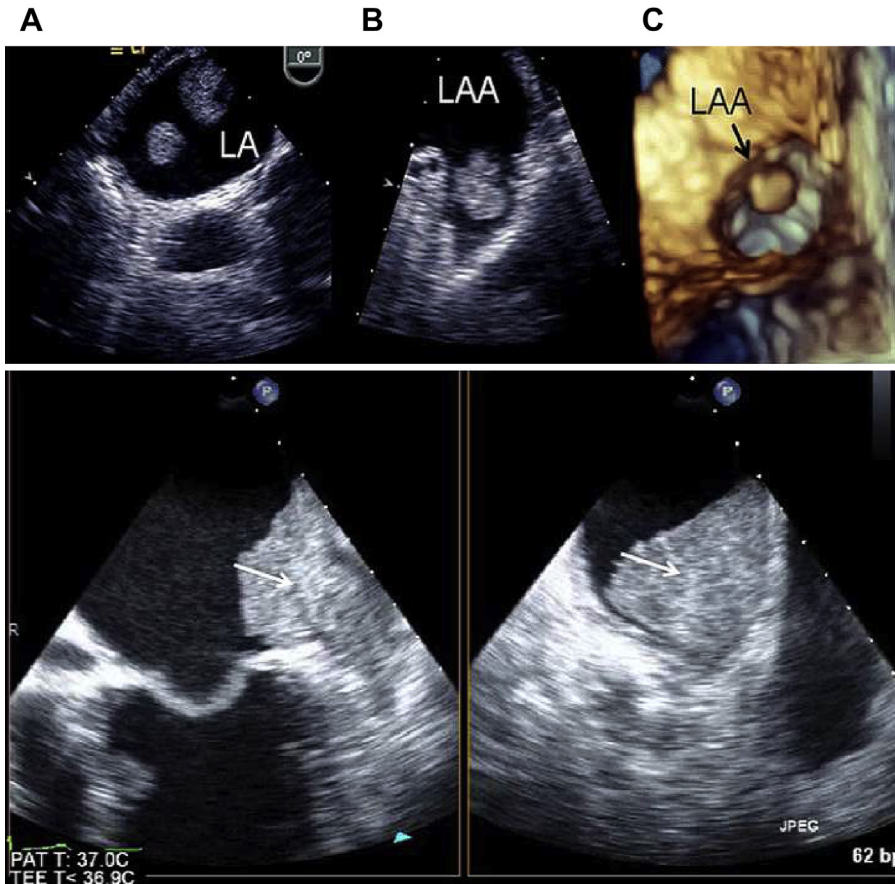


Fig. 4. (Top) In (A), 2 mobile thrombi are visible in 2D TEE (0°) in the left atrium (LA) of a patient with mitral stenosis before surgery. In (B), a large thrombus (2D TEE 70°) in the left atrial appendage (LAA) is shown, and in (C), a 3D TEE en face view of the LAA orifice reveals a thrombus close to the LAA ostium (arrow). (Bottom) 2D TEE x-plane images showing a large thrombus in the LAA (arrows).

MR.^{46,47} A TS approach (Fig. 11) is used to enter the left atrium and gain access to the MV. This catheter system has 2 arms that form a Clip when closed (see Fig. 10). During the procedure, the Clip arms are opened in the LV and during a pullback into the LA, the central portions of the MV anterior and posterior leaflets are entrapped in the Clip arms, creating a double mitral orifice (Fig. 12) and a reduction in MR. Box 3 lists echocardiographic parameters essential for evaluation before and during MitraClip placement.

Patient Selection

Patients with MitraClip often have comorbidities such as impaired LV function and reduced left ventricular ejection fraction (LVEF) ($<40\%$) that make them poor surgical candidates. Franzen and colleagues⁴⁸ showed that MitraClip implantation can be safely performed with good results even in patients with LVEF less than 20%.

For the MitraClip procedure, patients need to have moderate to severe or severe MR ($\geq 3+$ to 4+) (Table 6) and the appropriate MV morphology. As seen in Fig. 13A, there is P2 prolapse and flail with a flail gap that is not excessive. Fig. 13B shows severe functional MR with appropriate coaptation depth and normal leaflet morphology. Fig. 13C shows severe MR due to anterior leaflet prolapse with a trivial flail gap. Table 7 shows MV morphologic characteristics that identify optimal patients for MV Clip therapy.^{46,49}

Imaging of the MV

Echocardiography is the best method to assess MR severity, mechanism, reparability, and hemodynamic consequences.^{50,51} 2D TTE is used to assess MR severity, whereas TEE is used to assess valve morphology. Important 2D TEE views (Fig. 14) are used to characterize valve abnormalities. In the 0° views (from the upper esophagus),

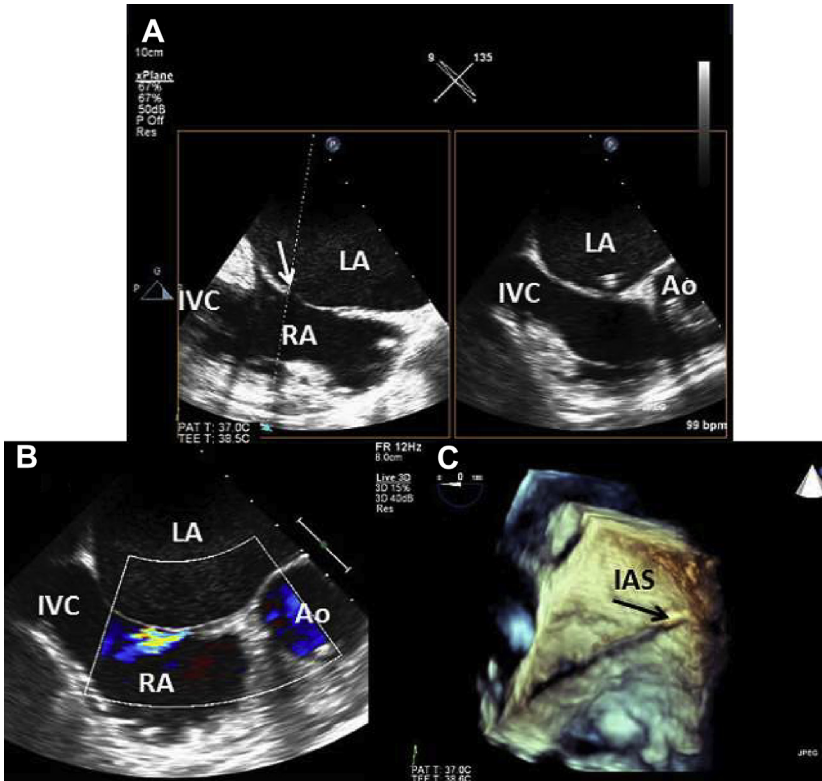


Fig. 5. (A) TEE x-plane image shows intraatrial septum (IAS; *white arrow*) from 2 aspects; the left panel shows the IAS in the long axis view with the inferior vena cava (IVC) to the left. The right panel identifies the aorta (Ao), an anterior structure, helping to avoid puncturing it by the transseptal (TS) needle. (B) Color flow in this view allows identification of a stretched patent foramen ovale (PFO) with left-to-right shunting. Puncture of the IAS at this site should be avoided (see text for more details). (C) 3D en face view of the IAS after the TS puncture and passage of the catheter and wire (*black arrow*). IVC, inferior vena cava; LA, left atrium; RA, right atrium.

A1 and P1 segments are seen in the superior position, A2 and P2 segments in the midesophagus, and A3 and P3 segments in the distal esophagus. In intercommissural views ($\sim 60^\circ$), the P1, A2, and P3 segments are seen when the plane cuts both commissures. With a clockwise rotation of the probe, the anterior leaflet segments A1 to 3 are seen, and with a counterclockwise rotation, the posterior leaflet segments P1 to 3 are seen. The left ventricular outflow tract (LVOT) view (additional 90° to the intercommissural view) demonstrates the A2 and the P2 segment. Transgastric short axis imaging shows all segments of both leaflets when optimal images are obtained.

3D TEE is superior to 2D for assessing mitral valve anatomy.^{50–53} X-plane imaging of the intercommissural view allows additional scanning of the valve segments from medial to lateral as well as assessment of the posteromedial and the anterolateral commissures as shown in **Fig. 13C**. 3D TEE provides detailed en face views

from the LA perspective (“surgical view”) of the mitral valve scallops. 3D images of the submitral apparatus from a ventricular view are especially helpful in assessing the anterior mitral leaflet as well as restricted posterior leaflet motion. In addition, 3D TEE is used to evaluate adjacent structures.⁵⁰

Posterior leaflet prolapses are best visualized from the LA view, and the anterior leaflet is also well seen from the LV (see **Fig. 13D**). Assessment of anterior prolapse (see **Fig. 13E, F**) can be more difficult than that of posterior prolapse (see **Fig. 13A, B**), as scallops are less pronounced on the anterior leaflet.⁵⁴ 3D TEE is more accurate in identifying which segments of the mitral valve are abnormal, prolapsed, or flail than 2D TEE.^{52–54} In addition, identifying perforations, clefts, and gaps is more accurate with 3D TEE.^{52,55}

In gated 3D echocardiography, multiple volumes are acquired (usually over 2–7 heart beats) and combined to form a single volumetric data

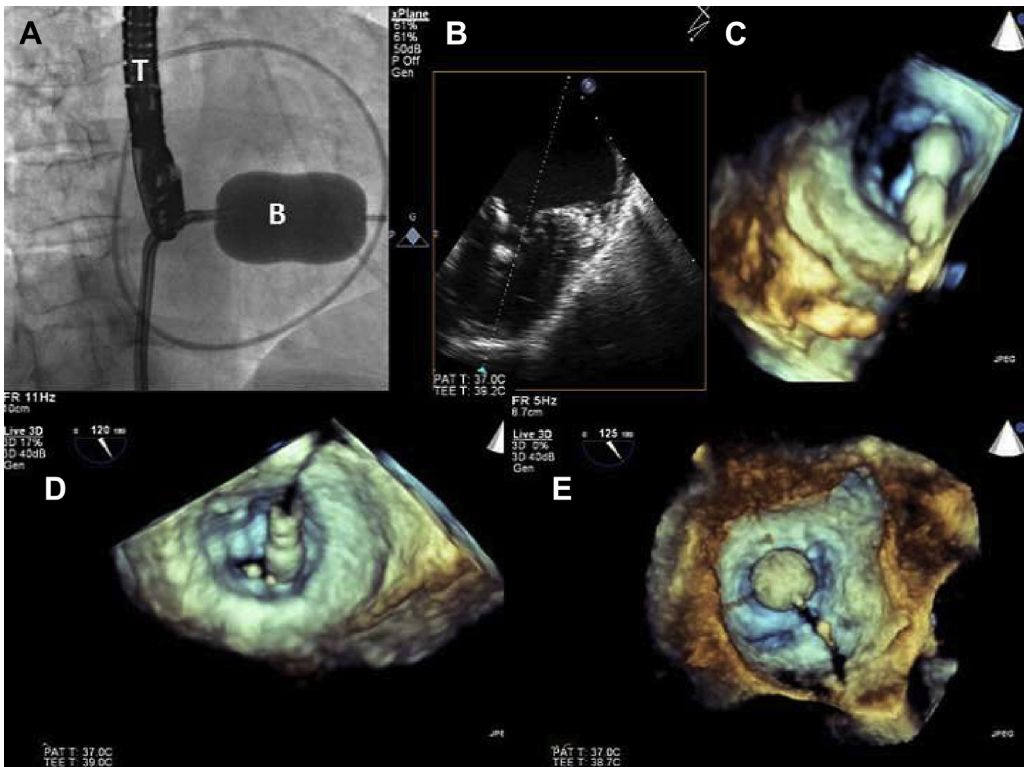


Fig. 6. (A) Fluoroscopy demonstrating TEE probe (marked T) and an inflated percutaneous mitral valvuloplasty balloon (marked B). (B) 2D TEE showing the balloon catheter across the mitral valve (MV). (C) An uninflated balloon is seen at the edge of the mitral orifice. (D) The balloon is seen entering the MV orifice. (E) The balloon is seen being inflated within the stenotic MV orifice.

set that has a higher temporal and spatial resolution. However, patient movement, respirations, or arrhythmias can cause artifacts with gated 3D imaging.⁵⁶

Guiding of the MitraClip Procedure

The MitraClip procedure is highly technical and is best performed when there is active collaboration and good communication between the echocardiologist and the interventionalist. 2D TEE can be used to guide MitraClip implantation; however, 3D TEE adds substantial information⁵⁷ regarding the position of catheters, wires, devices, and target structures in a single 3D view. 3D echo and x-plane imaging can optimize TS puncture, steering of the delivery catheter in a 3D space (LA) toward the mitral valve, and proper MitraClip positioning perpendicular to the line of coaptation in the middle segments of the mitral valve (see **Fig. 11**; **Figs. 15–20**). In one study, the addition of 3D TEE resulted in nearly a 30% reduction in procedure time⁵⁸ compared with 2D TEE and fluoroscopy.

As the initial intraprocedural evaluation of the MitraClip is done under general anesthesia, the type of anesthesia and the medications that influence preload and afterload should be kept constant to ensure that preprocedural, intraoperative, and postoperative assessments of MR are performed under similar hemodynamic conditions. For preprocedural and postoperative MR assessment, ultrasound settings including color scale and gain should be identical.

The MitraClip procedure is divided into 7 steps, which are outlined in **Box 4**.⁵⁹

Transseptal puncture

The optimal puncture site, located superiorly and posteriorly in the IAS, is determined by 2D TEE imaging planes: short axis view at the base for anterior-posterior orientation (30°–45°), a bicaval view for superior (cranial)-caudal orientation (90°–120°), and a 4-chamber view (0°–20°) to identify the height above the mitral valve for TS puncture. 3D x-plane allows imaging in a short axis view at the base and in a bicaval view simultaneously

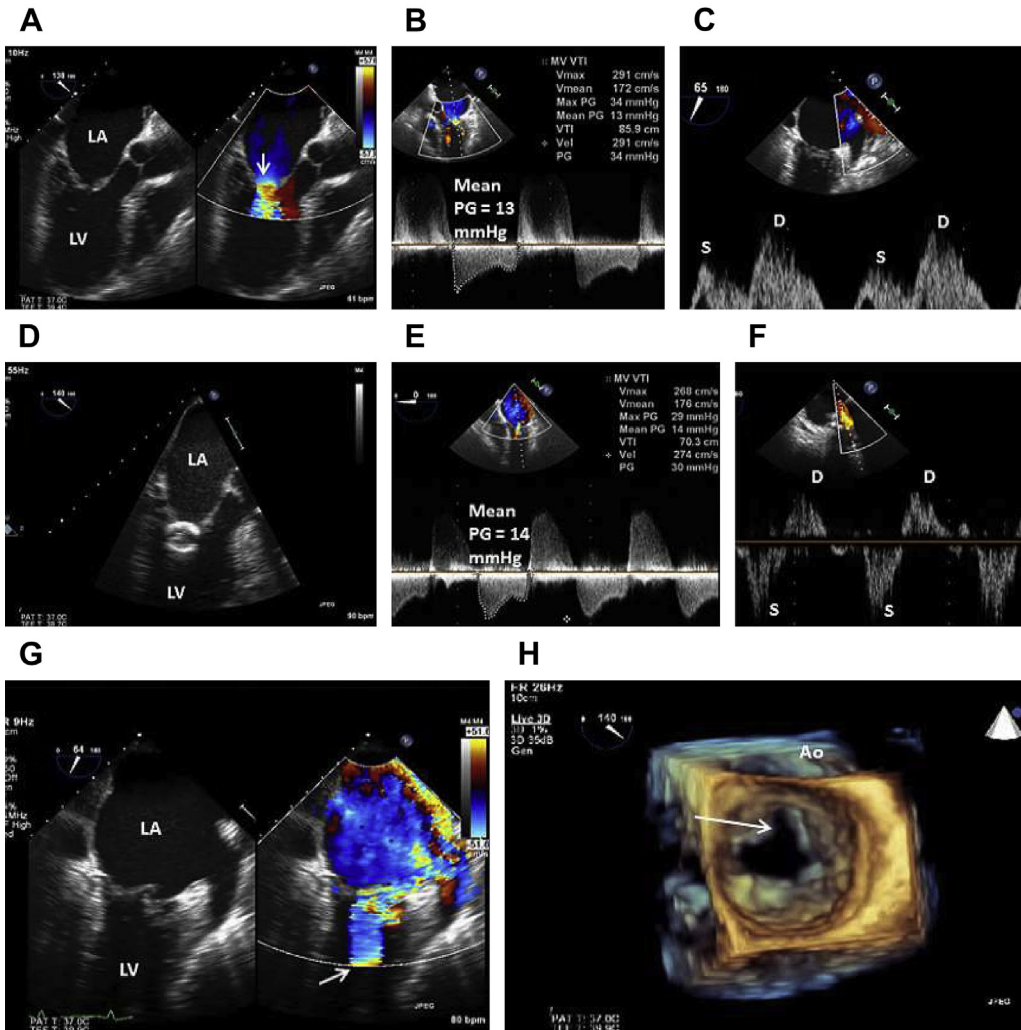


Fig. 7. (A) 2D TEE long axis view of a stenotic mitral valve; a diastolic PISA is present (*arrow*). (B) The mean diastolic pressure gradient (PG) is 13 mm Hg. (C) Doppler imaging of the pulmonary vein (PV) flow showing blunted systolic flow (marked S) and elevated diastolic flow (marked D), consistent with elevated left atrial filling pressures. (D) Percutaneous mitral valvuloplasty balloon is not at the valve level; rather it is too apical and inflated in the chordal apparatus. (E) The mean PG has gone up, the continuous wave Doppler now shows mitral regurgitation (MR) with a V-wave cutoff sign indicating acute MR. (F) There is associated systolic flow reversal in the PV. (G) A large PISA (*arrow*) in the left ventricle (LV) and severe eccentric, laterally directed, MR is shown. (H) 3D TEE in the surgical view of the left atrium (LA) shows that the anterior mitral leaflet, in addition to the commissures, has been split (*large arrow*). Ao, aorta.

(see **Fig. 11**). In cases with MV prolapse or flail MV (degenerative disease), the puncture site should be 4 to 5 cm above the mitral annulus to allow room for catheter and MitraClip system manipulation. With functional MR, the plane of MV coaptation is generally below the mitral annulus due to valve tethering. In these cases, the site of TS puncture is more apical, closer to the plane of the MV annulus, namely, ~ 3.5 cm above the annular plane. TS access should not be across a persistent

foramen ovale, as this site is too anterior. With suboptimal TS puncture site, the procedure is more difficult, complex, and generally takes longer due to the need for more catheter manipulations with the large MitraClip delivery system (CDS).

Introduction of the steerable guide catheter into the LA

The steerable guide catheter (SGC) is advanced with the dilator into the LA over a stiff guidewire,

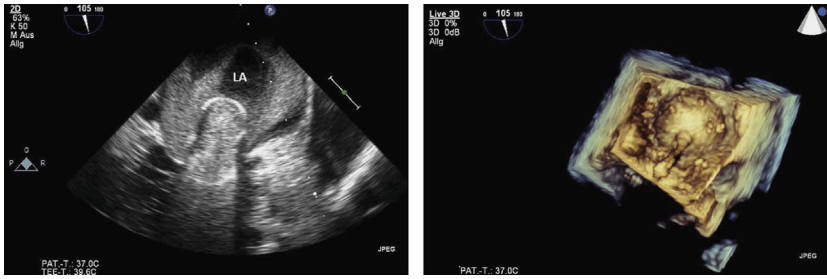


Fig. 8. (Left) 2D TEE showing the balloon being inflated within the stenotic MV orifice and the development of severe stasis in the left atrium (LA). (Right) 3D surgical view of the LA shows a fully inflated percutaneous mitral valvuloplasty balloon.

which is placed in the left upper pulmonary vein with fluoroscopic and TEE guidance (see **Fig. 15**). The dilator is identified by a cone-shaped tip with echogenic ridges. A radiopaque, echo bright,

double ring characterizes the tip of the guide catheter. To prevent damaging the LA wall, advancement of the SGC is done with continuous 2D and 3D TEE guidance and fluoroscopy (see **Fig. 15**).

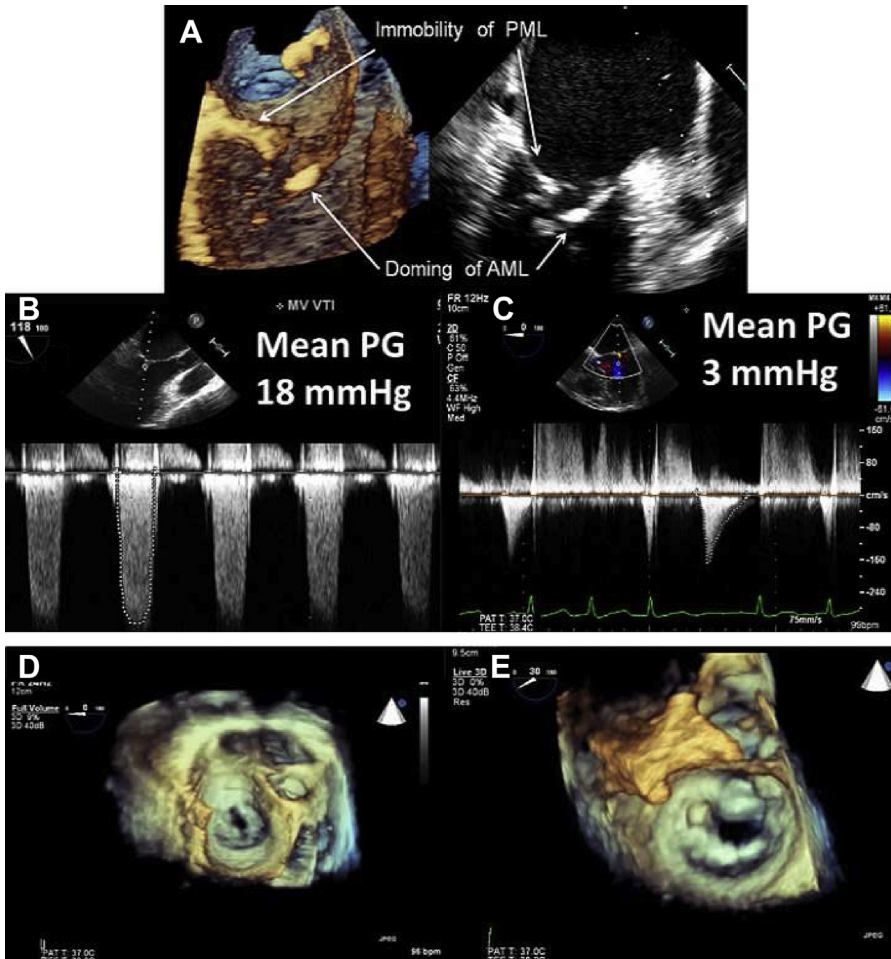


Fig. 9. (A) 2D and 3D TEE images post-balloon valvuloplasty. (B, C) Continuous wave Doppler showing the mean gradient (B) before and (C) after valvuloplasty, which has dropped from 18 to 3 mm Hg, indicating a successful procedure. (D, E) 3D images from the left atrium of the mitral valve orifice (D) before and (E) after successful valvuloplasty. AML, anterior mitral leaflet; PML, posterior mitral leaflet.

Table 5
Predictors of results after percutaneous mitral balloon valvuloplasty

Predictors of Good Immediate Results	Predictors of Good Long-term Results
Commissural calcium grade 0/1 ^{27,28}	Complete commissural opening ³⁹
Wilkins score <8 ^{3,23}	Larger MV area post-PMBV ³⁹
Presence of sinus rhythm ⁶	Presence of sinus rhythm ⁴⁰
Good leaflet mobility ³¹	Absence of calcium at fluoroscopy ⁴⁰
No involvement of the subvalvular apparatus ³¹	Low MR grade after PMBV ⁶
	Wilkins score ≤ 8 ³²
Predictors of Poor Immediate Results	Predictors of Poor Long-term Results
Older age ^{1,30}	Higher cardiothoracic index ³⁰
Smaller initial MV area ^{1,30}	Lower MV area post-PMBV ³⁰
Use of the double-balloon technique ³⁰	Previous open heart (surgical) commissurotomy ^{30,41}
Higher echocardiographic group ³⁰	Immediate post-PMBV mean PAP (cutoff >25 mm Hg) predicts mitral reintervention ⁴²
Commissural calcium grade 2/3 ^{27,28}	Increasing preprocedural and postprocedural MR ⁴³
Wilkins score >8 ^{3,23}	Wilkins score >8 ^{32,41}
Valvular calcification and severe subvalvular lesions ³	Post-PMBV mitral regurgitation ≥ 3 ⁴¹
Previous commissurotomy ¹	Older age ⁴⁴
Baseline mitral regurgitation ¹	NYHA functional class IV ⁴¹
	Pre-PMBV mitral regurgitation ≥ 2 ⁴¹
	Higher post-PMBV pulmonary artery pressure ⁴¹

Abbreviation: PAP, pulmonary artery pressure.

After the SGC is in the LA, the dilator and guidewire are removed.

Advancement of the clip delivery system into the LA

The CDS is placed in the LA under fluoroscopic guidance (see **Fig. 16**). 2D and 3D TEE monitoring are also used to maintain the end of the SGC across the IAS. The location of the CDS and the Clip are imaged continuously to ensure that the tip does not cause injury to the free LA wall. 3D TEE and x-plane imaging are useful to assess the distance of the CDS from the LA wall.

Box 2

Role of echocardiography during percutaneous mitral balloon valvuloplasty

- Reassessment of mitral valve pathology before the procedure (MS and MR) and identification of contraindications (see **Box 1**)
- Guidance of transseptal puncture
- Optimization of balloon placement across the MV orifice
- Assessment of residual MS after PMBV
- Assessment of MR severity after PMBV
- Assessment of complications

Steering and positioning of the MitraClip above the mitral valve

The positioning of the CDS above the mitral valve is best guided by 3D TEE. On 2D TEE medial-lateral Clip adjustments are monitored in the midesophageal intercommissural view and anterior-posterior adjustments in the orthogonal midesophageal long axis view (see **Fig. 17**). The MitraClip needs to be positioned in the LA at the mid portion of the MV leaflets and perpendicular to the line of MV coaptation. This is difficult to confirm with 2D TEE but straightforward with 3D TEE. The MitraClip should also split the regurgitation jet in both orthogonal views, and the tip of the Clip should be directed toward the largest proximal isovelocity surface area (PISA). A short axis trans-gastric view is used to assess Clip orientation when only 2D TEE imaging is available, as 3D TEE en face view generally allows precise orientation of the MitraClip arms in the LA. As shown in **Fig. 17**, the 3D en face view identifies when the Clip is positioned above the middle segments of the MV and oriented perpendicular to the line of MV coaptation.

Advancing the MitraClip into the LV

Advancing the MitraClip with the Clip arms open into the LV is well seen by fluoroscopy and with x-plane imaging in which the intercommissural view (60° – 90°) and the LVOT view (110° – 130°)

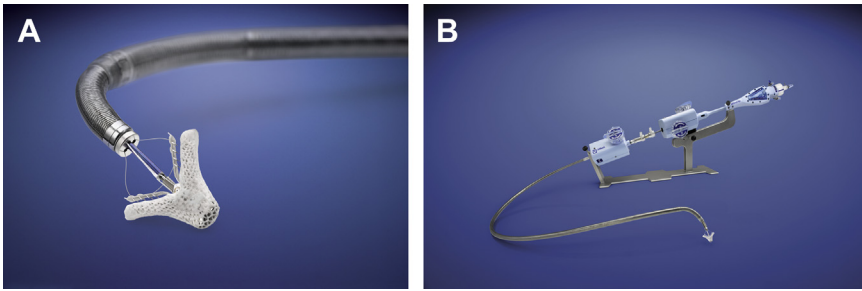


Fig. 10. (A) A close-up view showing the Teflon-covered MitraClip arms; the gripper arms are seen below. (B) The entire catheter delivery system is shown, and it includes the platform on which the catheter sits during the procedure, the anterior-posterior (A/P) knob, and the mediolateral (M/L) knob. The MitraClip is a 22F system, which fits inside a 24F catheter system. (Courtesy of Abbott Vascular, Santa Clara, CA; with permission. CAUTION: Investigational device. Limited by Federal (U.S.) law to investigational use only.)

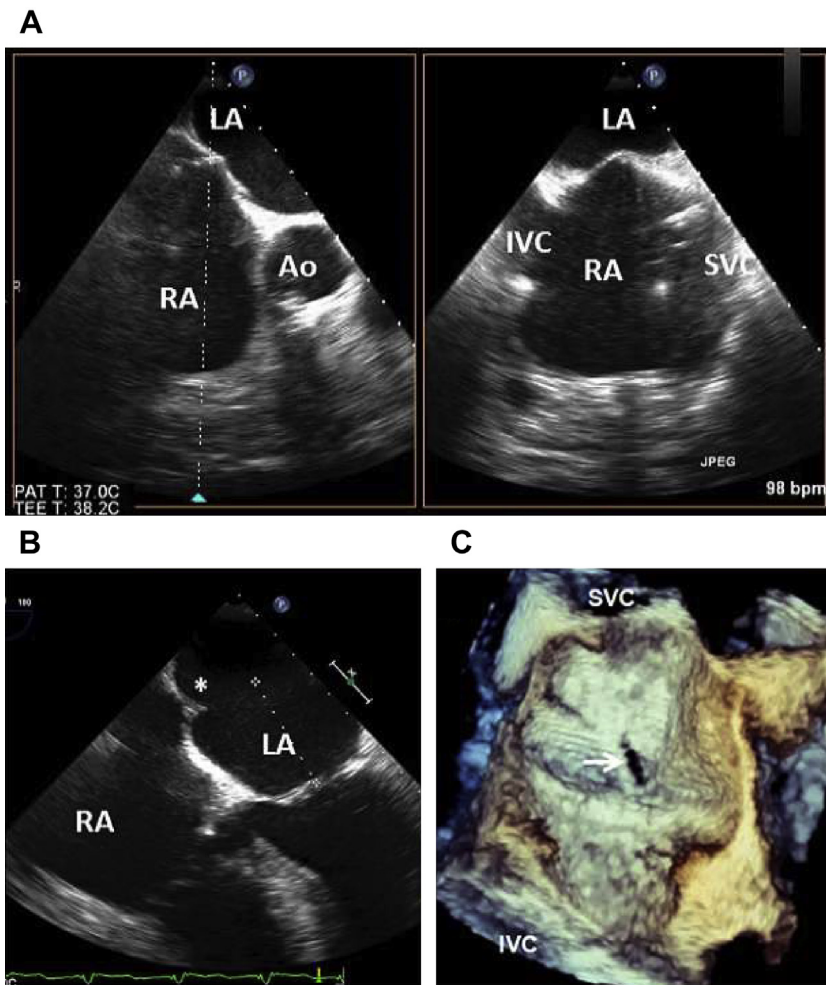


Fig. 11. (A) 2D TEE x-plane view of the intraatrial septum (IAS); the aorta (Ao) is anterior, the inferior vena cava (IVC) is caudal, and the superior vena cava (SVC) is cephalad. (B) The distance from the transeptal (TS) needle to the mitral annular plane is measured for optimal TS puncture site for the MitraClip (*asterisk*). It is more superior (≥ 4 cm) in degenerative mitral regurgitation (MR) and more apical (3.5–4 cm) with functional MR. Indentation from the TS needle (*asterisk*) is shown as in a (C) 3D en face view of the left atrium (LA) showing a left atrial aspect of the IAS immediately after a MitraClip procedure (*white arrow* marks the slitlike residual IAS defect after the TS puncture). RA, right atrium.



Fig. 12. 3D TEE images of the mitral valve after the MitraClip procedure from the atrial (top) and ventricular (bottom) views. Note the double orifices (asterisk). AML, anterior mitral leaflet; Ao, aorta; LA, left atrium; LVOT, left ventricular outflow tract; PML, posterior mitral leaflet.

Box 3

Echocardiographic parameters essential for evaluation before, during, and after MitraClip implantation

- Quantification of mitral valve morphology and MR severity
- Guidance of the MitraClip system during the procedure
- Assessing intraprocedural results
- Identification of complications during the procedure
- Assessment of final results post-Clip implantation in regard to MR severity and diastolic gradient
- Follow-up regarding MR severity, residual shunting through the atrial septum at the site of transeptal puncture, and pulmonary artery systolic pressure

are simultaneously visualized (see **Fig. 18**). The LVOT view is used to demonstrate and locate the open Clip arms. With the intercommissural view, no parts of the Clip arms should be seen. As demonstrated in **Fig. 18**, fluoroscopy and TEE guide the device across the MV into the LV, where orientation of the Clip arms and CDS are reassessed. As the guiding catheter and Clip may rotate during advancement from the LA to the LV, as shown in **Fig. 18**, 2D transgastric short axis view or 3D imaging from either the LA or the LV is used to reassess the Clip orientation in relation to the mitral valve and the line of coaptation. Using an en face LA view, the gain should be lowered to visualize the Clip in the LV and its orientation relative to the MV.

Grasping of the leaflets and assessment of proper leaflet insertion

As demonstrated in **Fig. 19A**, leaflets are usually grasped using the 2D LVOT view (see **Fig. 19**). The MitraClip is initially closed up to 60°–90°. Full closure is done after demonstrating that there is adequate insertion of both the anterior and posterior leaflets and a reduction in MR severity. Multiple imaging planes are used to assess leaflet insertion. As found in **Fig. 19A**, the posterior leaflet insertion is well seen in the LVOT view, and the anterior and posterior leaflet insertions are well seen in the 4-chamber view (see **Fig. 19B**). Slight rotations of the TEE probe are used to view the leaflet insertion from different angulations. The intercommissural view may help detect chordae tendinae that are entrapped within the Clip. After echo documentation that the leaflets are well inserted and positioned within the Clip and gripper arms along with a reduction in MR, the MitraClip is fully closed.

Assessment of result and MitraClip release

With each MitraClip procedure, the maximal possible reduction of MR should be strived for without creating residual MS (see **Fig. 20**; **Fig. 21**). Confirmation that both leaflets are adequately grasped and inserted in the MitraClip is essential. Placement of a MitraClip creates a tissue bridge between the two leaflets, which separates a medial and a lateral orifice. Identified in **Fig. 20**, the final orifice size and geometry can be evaluated in 3D en face aspects of the mitral valve from the left atrium and the left ventricle. An isosceles tissue triangle indicates uniform and symmetric placement of the MitraClip on both leaflets.

Qualitative and quantitative assessment of MR severity can be difficult due to the double mitral valve orifice (or triple orifice in some cases in which 2 Clips are implanted). There are no validated

Table 6
Assessment of MR severity

	Mild	Moderate	Severe
Qualitative			
MR color flow Doppler	Small central jet <4 cm ² or <20% of LA volume	Signs of MR > mild but no criteria for severe MR	Large central jet >40% of LA volume/eccentric wall hugging jet
Proximal isovelocity (PISA)	No or minimal PISA	Signs of MR > mild but no criteria for severe MR	Large PISA
CW Doppler signal of MR jet	Non-echo dense/parabolic	Echo dense/parabolic	Dense/late systolic cutoff
Semiquantitative			
Vena contracta width (cm)	<0.3 cm	Signs of MR > mild but no criteria for severe MR	≥0.7 cm
Pulmonary vein flow	Systolic dominant flow	Intermediate signs	Blunted S-wave or systolic flow reversal
Mitral inflow	Dominant A-wave	Intermediate signs	Dominant E-wave (>1.2 m/s)
LA/LV size	Normal LV size	Intermediate signs	Enlarged LA and/or LV
Quantitative			
Regurgitant volume (R Vol) (mL/beat)	<30	Mild-moderate: 30–44 Moderate-severe: 45–59	≥60
Regurgitant fraction (%)	<30	Mild-moderate: 30–39 Moderate-severe: 40–49	>50
Effective regurgitant orifice area (cm ²)	<0.2	Mild-moderate: 0.2–0.29 Moderate-severe: 0.3–0.39	≥0.4

studies or guidelines to grade severity of residual MR after Clip implantation. The authors use color flow, pulsed wave, and CW Doppler in concert to assess residual MR.^{10,11,50}

At least trivial residual MR is always present post-MitraClip implantation. Color jet area is larger with multiple jets, commonly seen after a MitraClip procedure. There is potential to overestimate residual MR with multiple jets.⁶⁰ As the MitraClip is echo dense, it can cause artifacts and affect assessment of residual MR. The presence of small color jets, even if multiple, is generally consistent with mild MR.

Hemodynamically significant MR reduction reduces LA pressure. As seen in **Fig. 21**, pulmonary vein systolic flow reversal (if present pre-Clip) disappears and the S-wave should become more pronounced or even dominant with a successful Clip procedure.

Vena contracta and PISA methods have not been validated to assess MR severity post-MitraClip due to multiple jets and affected MV

orifice. Regurgitant volume in the absence of aortic regurgitation and ventricular septal defects can be calculated by subtracting the forward flow (velocity-time integral derived in the LVOT × LVOT area) from the total stroke volume (end-diastolic volume – end-systolic volume) for quantification of MR.⁶¹ For LV volumes, 3D acquisition is reported to be superior to 2D.⁵⁷ Recent studies indicate that 3D echo has potential to quantify MR in the presence of irregularly shaped vena contracta areas; however, this needs further validation.^{62,63} Evaluation of the severity of residual MR is supplemented by the catheterization laboratory data. With a reduction in MR, there is a decline in the LA or pulmonary capillary wedge pressure (PCWP) V wave, improved stroke volume, and reduced MR by contrast left ventriculography.

The mitral valve gradient is evaluated after each MV Clip to prevent the creation of significant MS. A transvalvular mean gradient of 5 mm Hg or less by CW Doppler is acceptable. Planimetry of the new orifices is done with 2D or standard transgastric

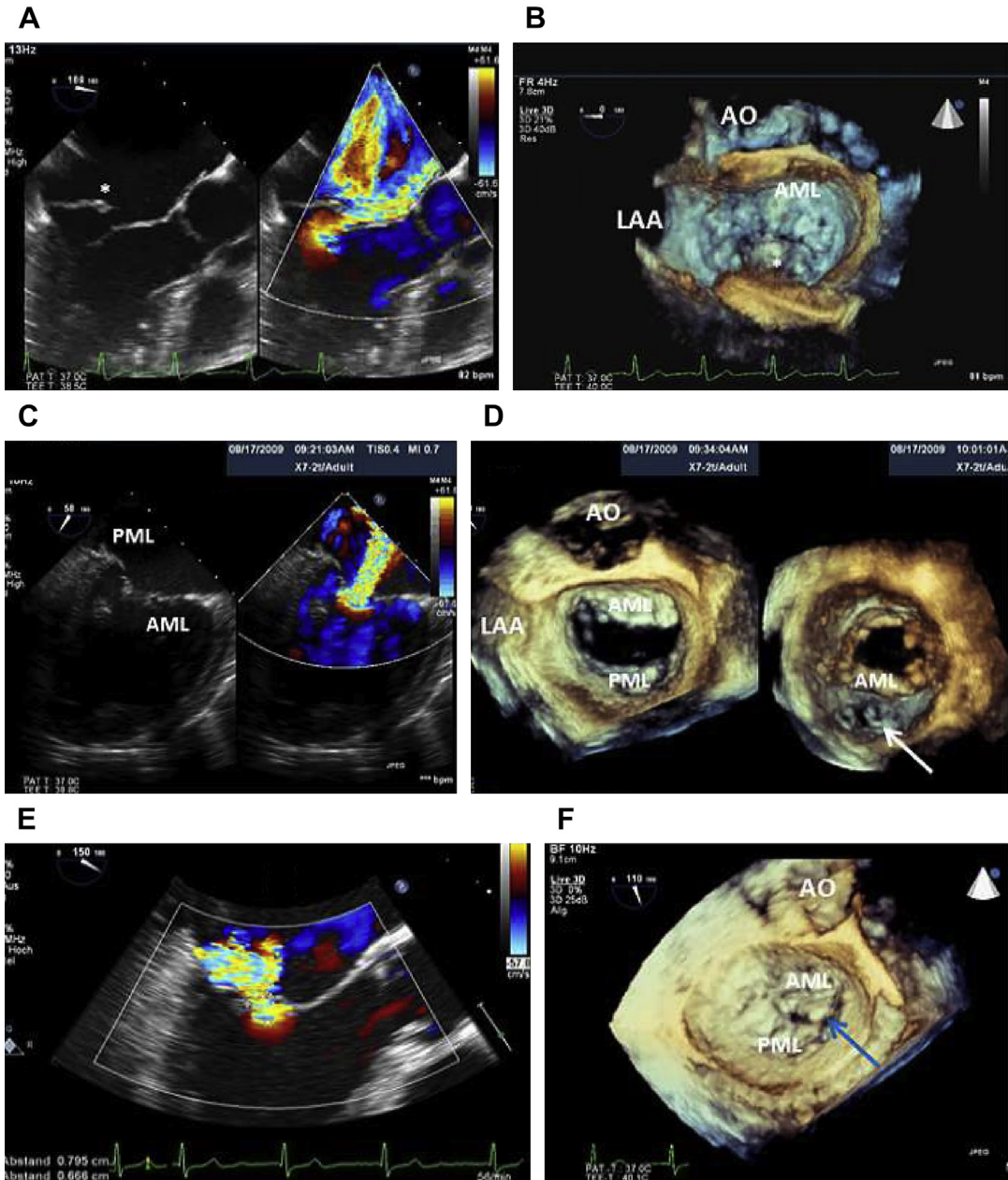


Fig. 13. (A) 2D TEE showing a flail posterior mitral leaflet (PML, *asterisk*) and severe mitral regurgitation (MR) confirmed by (B) 3D TEE demonstrating a flail midportion of the posterior leaflet (P2) (*asterisk*). (C) 2D TEE showing a dilated globular left ventricle and severe central MR. (D) 3D TEE confirms normal mitral valve leaflet morphology, but the LV 3D view suggests some restriction of the PML (*arrow* pointing at the left ventricular outflow tract). (E) 2D TEE long axis view showing severe MR with a large PISA and vena contracta and a posteriorly directed jet. (F) 3D TEE confirms prolapse of the anterior mitral leaflet (AML, *blue arrow*). Ao, aorta; LAA, left atrial appendage.

short axis view 3D TEE. If the sum of the planimetered orifices gives an area of less than 1.5 cm^2 , this is criteria for significant MS.^{46,49} After MitraClip deployment, there does not seem to be progression of MS based on a 2-year follow-up study.^{64,65}

In cases with greater than 2+ MR, an additional Clip may be placed if the gradient is less than 3 to 4 mm Hg or the Clip can be moved to a more optimal site. After Clip deployment, MR needs to be reassessed as changes in MR can occur after

Table 7
Morphologic characterization for MitraClip eligibility

Ideal Valve Morphology for a MitraClip Procedure	Unsuitable Valve Morphology for a MitraClip Procedure
MR originating from the midportion of the valve (degenerative or functional etiology)	Perforated mitral leaflets or clefts Lack of primary and secondary chordal support
Lack of calcification in the grasping area	Severe calcification in the grasping area
Mitral valve area $>4 \text{ cm}^2$	Hemodynamically relevant mitral stenosis
Length of posterior leaflet $\geq 10 \text{ mm}$	Length of posterior leaflet $<7 \text{ mm}$
Nonrheumatic or endocarditic valve disease	Rheumatic valve disease—with restriction in systole and diastole (Carpentier IIIa) or endocarditic valve disease
Flail width $<15 \text{ mm}$ Flail gap $<10 \text{ mm}$	
Sufficient leaflet tissue for mechanical coaptation: Coaptation depth $<11 \text{ mm}$ Coaptation length $>2 \text{ mm}$	Gap between the leaflets $>2 \text{ mm}$

Adapted from the EVEREST criteria and the Abbott training center experience.

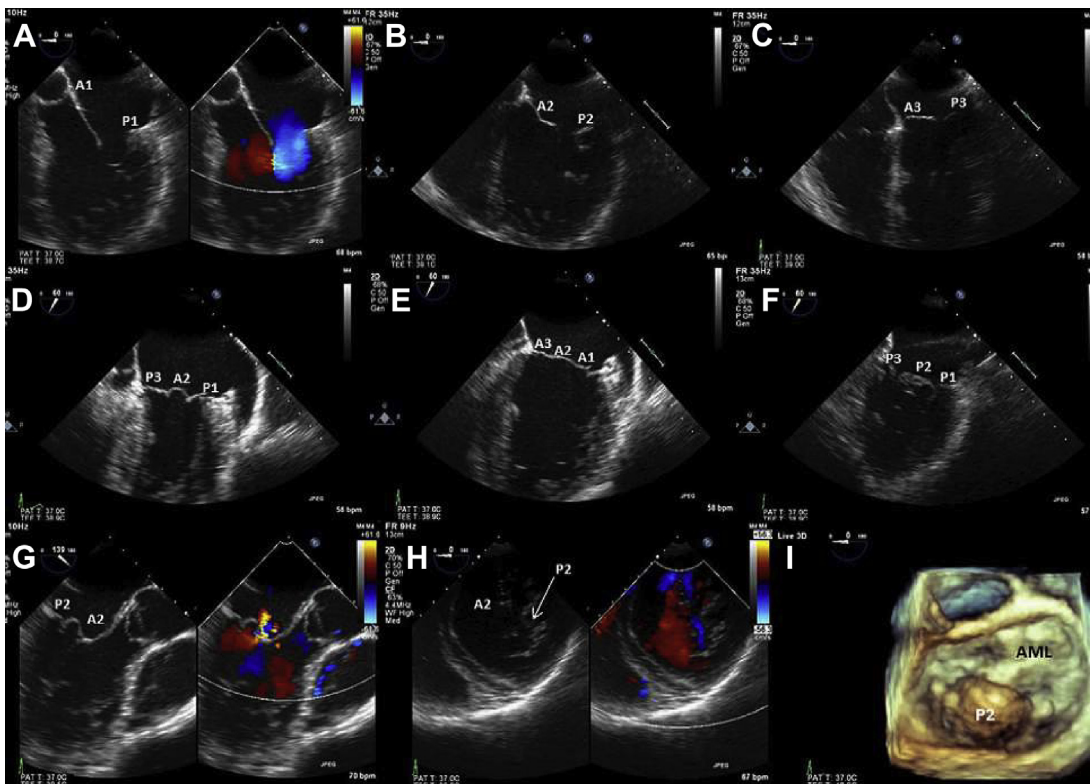


Fig. 14. 2D TEE imaging to evaluate mitral regurgitation (MR) morphology. Panels (A–C) show each segment of the anterior and posterior leaflet as described in the text. In the 5- and 4-chamber views, (D–F) show the bicommisural view for evaluating the anterior leaflet when the transducer is rotated clockwise and counterclockwise to bring out the leaflets. (G) Long axis 3-chamber view demonstrates clearly the midportion of the anterior and posterior leaflet (A2, P2). (H) The transgastric view demonstrates all segments of the anterior and posterior leaflets as well as the line of coaptation (arrow pointing to P2). (I) A single 3D TEE view demonstrates that it can be used to supplant the multiple imaging planes of 2D to identify the prolapsed middle scallop of the posterior leaflet.

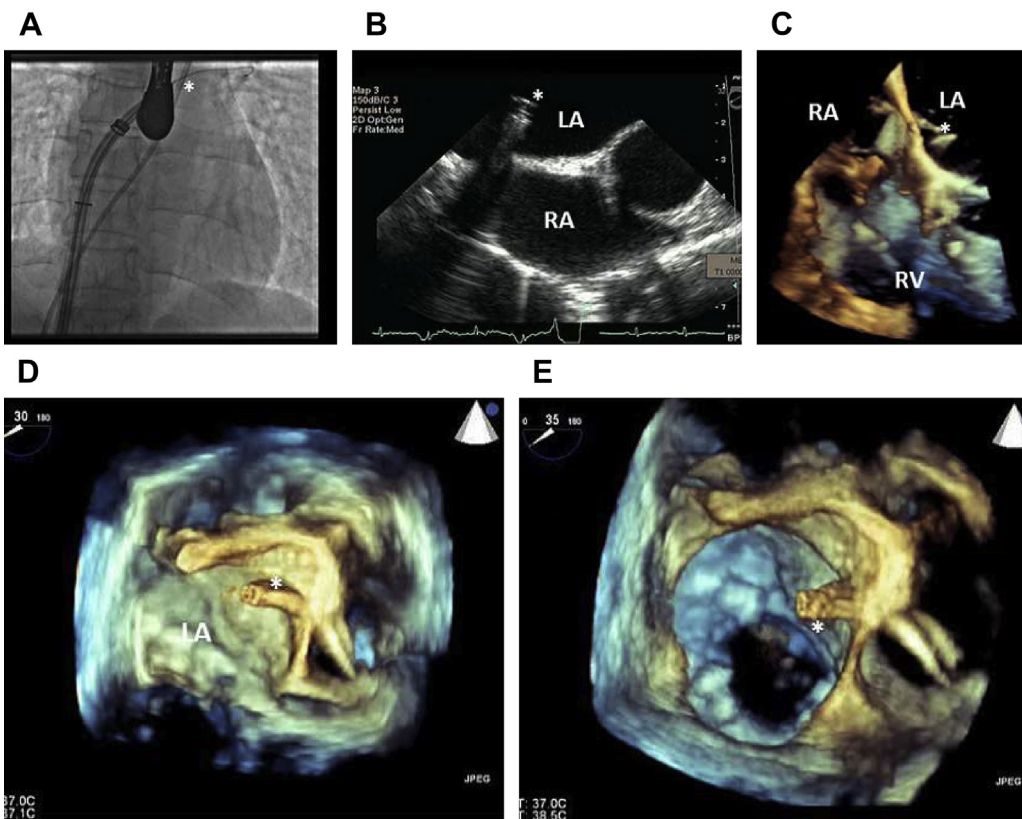


Fig. 15. (A) Fluoroscopic, (B) 2D TEE, and (C–E) 3D TEE images show advancement of the guide catheter (asterisk) into the left atrium (LA). RA, right atrium; RV, right ventricle.

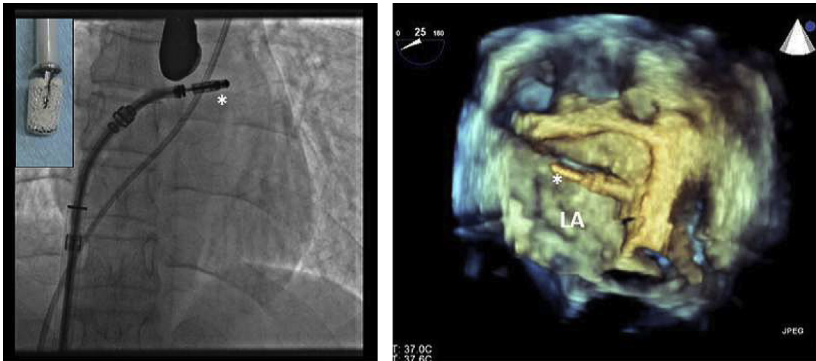


Fig. 16. (Left) Fluoroscopy and (right) 3D TEE show the advancement of the MitraClip (upper left box) into the left atrium (LA).

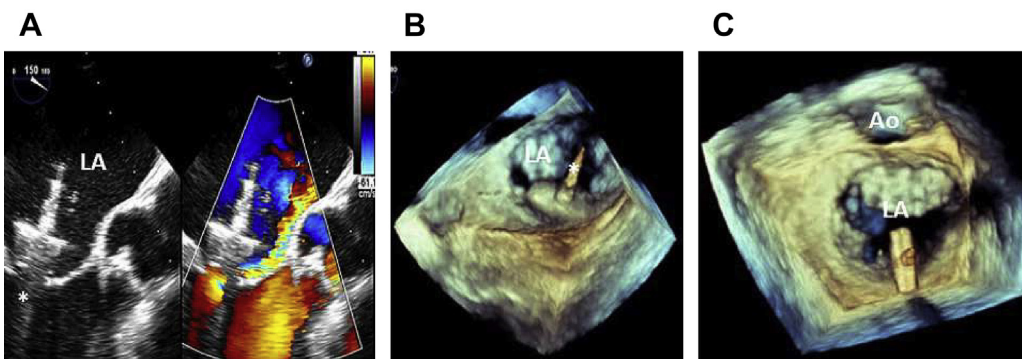


Fig. 17. (A) 2D TEE and (B, C) 3D TEE showing the MitraClip (asterisk) in the left atrium (LA). (B) The MitraClip is not in the midportion of the mitral valve (MV) or perpendicular to the MV line of coaptation. (C) After catheter manipulation, the Clip is now perfectly aligned. Ao, aorta.

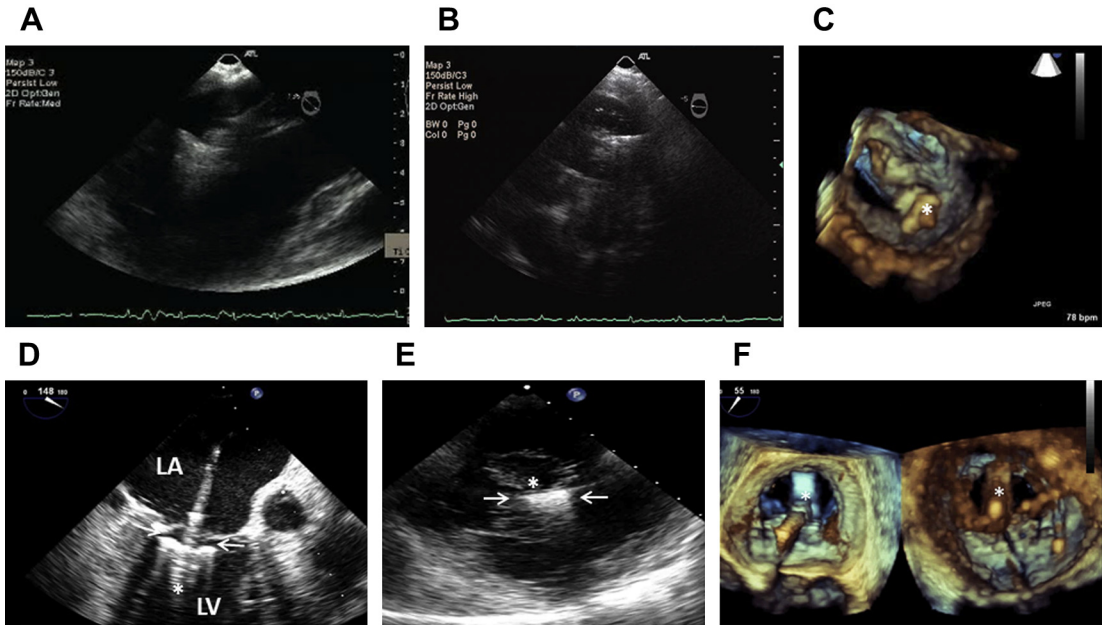


Fig. 18. The Clip (*asterisk*) is shown advanced into the left ventricle (LV) by (A, B) 2D TEE and (C) 3D TEE. (B) 2D TEE short axis view and (C) 3D view from the LV, which show the Clip to be perpendicular to the MV line of coaptation. (D) Long axis TEE view showing the valve at the time of grasping of the leaflets. (E) Short axis view and (F) 3D TEE also showing grasping of the anterior and posterior mitral valve leaflets (*arrows* show clip and leaflets in contact). LA, left atrium.

the Clip is released as the tension on the MV and the Clip changes when the CDS is released.

Additional MitraClip Implantation

During placement of a second MitraClip, its orientation in the LA is optimized by 2D or 3D echocardiography. The Clip is closed before advancing into the LV to avoid any interference or entanglement with chordae tendinae. The Clip is reopened in the LV. Fluoroscopy is helpful in positioning of a second MitraClip, as it should be aligned as parallel as possible to the first Clip. Entrapment of leaflet tissue between 2 MitraClips should be avoided, as this may cause uncorrectable residual MR.

ASSESSMENT OF COMPLICATIONS

The MitraClip is a safe procedure with low morbidity and mortality.^{46,48,49} The most frequent complications are listed in **Table 8**.

PARAVALVULAR MITRAL LEAKS

The development of a PVL following cardiac valve surgery is one of the most frequent causes for reoperation.⁶⁶ It is generally due to a dehisced

suture or a complication of infected endocarditis. Sixty percent of PVLs occur in the first year after surgery,⁶⁷ with subsequent risk decreasing to between 0.06% and 5.4%.^{68–72}

PVLs can be isolated, or multiple, and can occur in association with any valve type.^{44,73–82} Most of the leaks remain small and asymptomatic⁸³ and even spontaneous closure of PVLs has been described, induced by fibrosis of the valve annulus.⁸⁴

Clinically significant PVLs after surgical valve replacement are reported to occur in 1% to 5% of patients.^{85–88} Clinically relevant PVMLs occur most frequently in association with mechanical mitral prostheses, and they are located most frequently in the mitral commissural areas (76%).^{83,89,90}

TEE for localizing and closing PVLs is critical. 3D TEE is the optimal way to assess a PVL preprocedure, intraprocedure, and postprocedure.^{91–94}

3D assessment in real-time provides en face views of the cardiac valves, allowing complete and adequate evaluation of the 3D character of PVLs in a single view. The size of the defects and location with respect to surrounding cardiac structures can usually be identified. This information is crucial for determining the approach, as well as device size and shape for closure. 3D TEE evaluation of such leaks often demonstrates

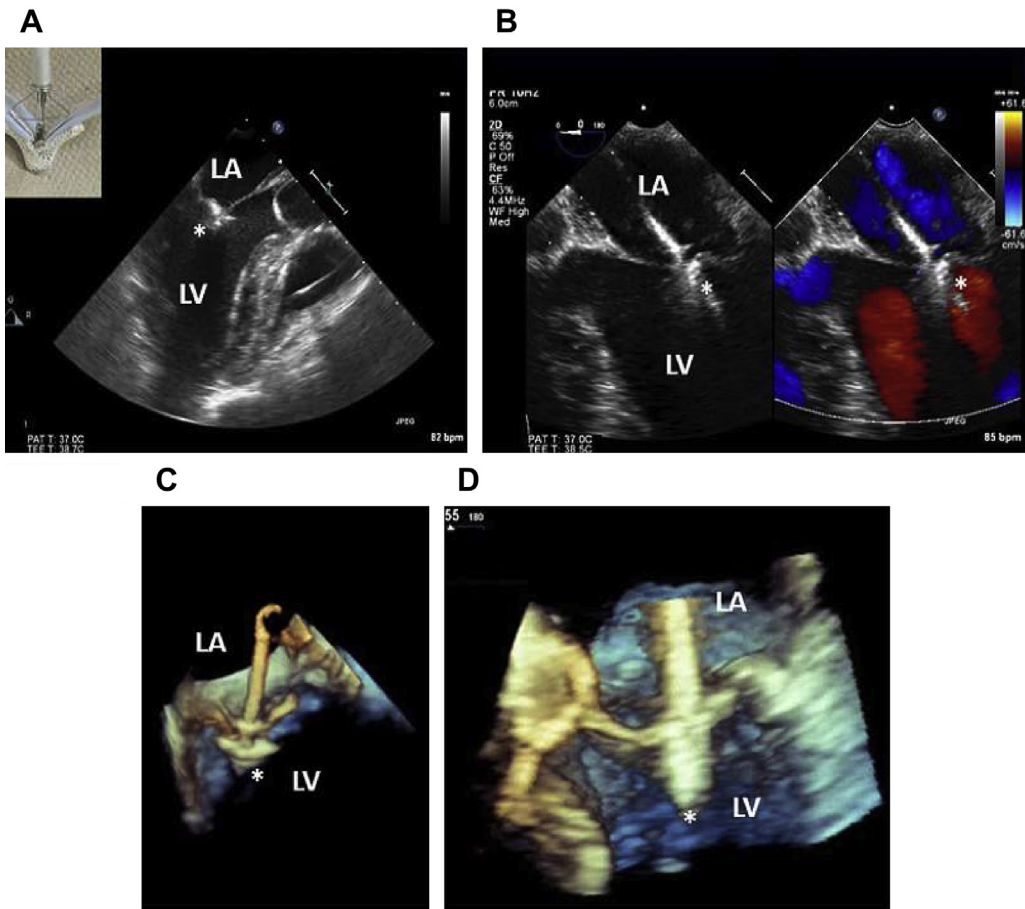


Fig. 19. (A) 2D TEE long axis view and (B) 4-chamber view during grasping of the mitral valve leaflets. The posterior leaflet insertion is well seen in (A and B), and the anterior leaflet insertion is better seen in the 4-chamber view. The 3D images (C, D) also confirm insertion of both leaflets. LA, left atrium; LV, left ventricle. A photo example of an open MitraClip is shown in the left upper box in (A). Asterisks represent the tip of the MitraClip in the LV.

oval or slitlike lesions and a larger extent of the defect than is seen by conventional 2D TEE.

Surgical repair of PVLs had been the standard treatment. However, as shown in **Table 9**, there is substantial increase in mortality and recurrence of PVLs with each reoperation.^{95,96}

The first successfully performed percutaneous PVL closure was reported in 1992 by Hourihan and colleagues.⁹⁷ They used a double-umbrella Rashkind occluder device in 7 patients.

Case reports and small series that used a broad spectrum of different devices (the most frequently used are listed in **Table 10**) documented variable clinical outcomes (54%–100%) and technical success rates in a range from 63% to 100%.^{85,98–106}

PARAVALVULAR MITRAL LEAK CLOSURE

Preprocedural Assessment

TEE is mandatory to identify the PVLs and to characterize the location, number, and shape of the PVLs, as paravalvular MR may be missed on TTE because of artifacts and reverberations caused by MV prosthesis. The leaks typically have an irregular shape.^{107–109} An assessment in multiple angles including off-axis views is crucial to determine the exact location and severity of the regurgitation. The characteristic feature of a PVL is a color Doppler flow jet outside of the sewing ring of the implanted valve. To define the severity of a PVML, the MR jet width at its origin is measured. Vitarelli and colleagues¹¹⁰ suggested 1 to 2 mm

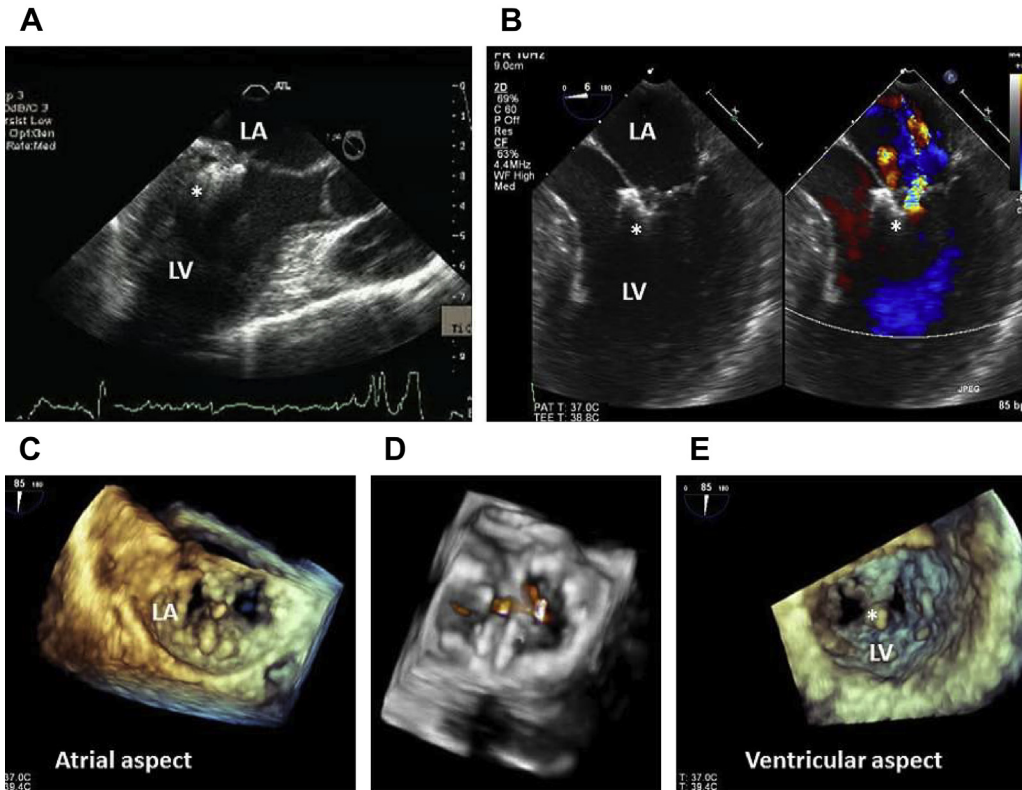


Fig. 20. Images obtained postdeployment of the MitraClip (asterisk). (A) 2D TEE long axis view shows the Clip connecting the anterior and posterior mitral leaflets, also seen in the (B) 5-chamber view. (C–E) 3D TEE showing the Clip from the (C, D) atrial aspect and minimal mitral regurgitation and (E) showing the double orifice after the Clip deployment. LA, left atrium; LV, left ventricle.

for mild, 3 to 6 mm for moderate and greater than 6 mm to define a severe PVL. A multimodal approach including semiquantitative and quantitative parameters similar to those used for the evaluation of native valves^{10,11,50} is also used, but the jets are frequently eccentric, thus, complicating assessment and quantification.

Box 4 Major steps for MitraClip implantation

1. TS puncture
2. Introduction of the steerable guide catheter into the LA
3. Advancement of the Clip delivery system into the LA
4. Steering and positioning of the MitraClip above the mitral valve
5. Advancing the MitraClip into the LV
6. Grasping of the leaflets and assessment of proper leaflet insertion
7. Clip detachment

3D TEE improves the detection, location, and assessment of shape and size of PVMLs as well as guidance for PVML closure.^{111–113} TEE plays an essential role during PVML closure by guiding the preferred TS puncture site, facilitating passage of wires and catheters across the PVML, providing navigation of catheters and guides in the LA or LV to approach the PVMLs, verifying correct canalization of the target lesions, sizing the defect, and positioning of the devices before deployment. A comprehensive evaluation of the procedural outcome includes the confirmation of normal mechanical valve function after device placement, the assessment of residual PV leakage, and the prompt detection of complications. The additional information rendered by 3D TEE (more precise evaluation of location and extent of the defects; facilitated wire, catheter, and device maneuvering and positioning; and a more comprehensive assessment of PVML severity postprocedure) may help avoiding complications such as suboptimal occluder alignment, malpositioning, or interference with neighboring structures and may shorten procedure times.

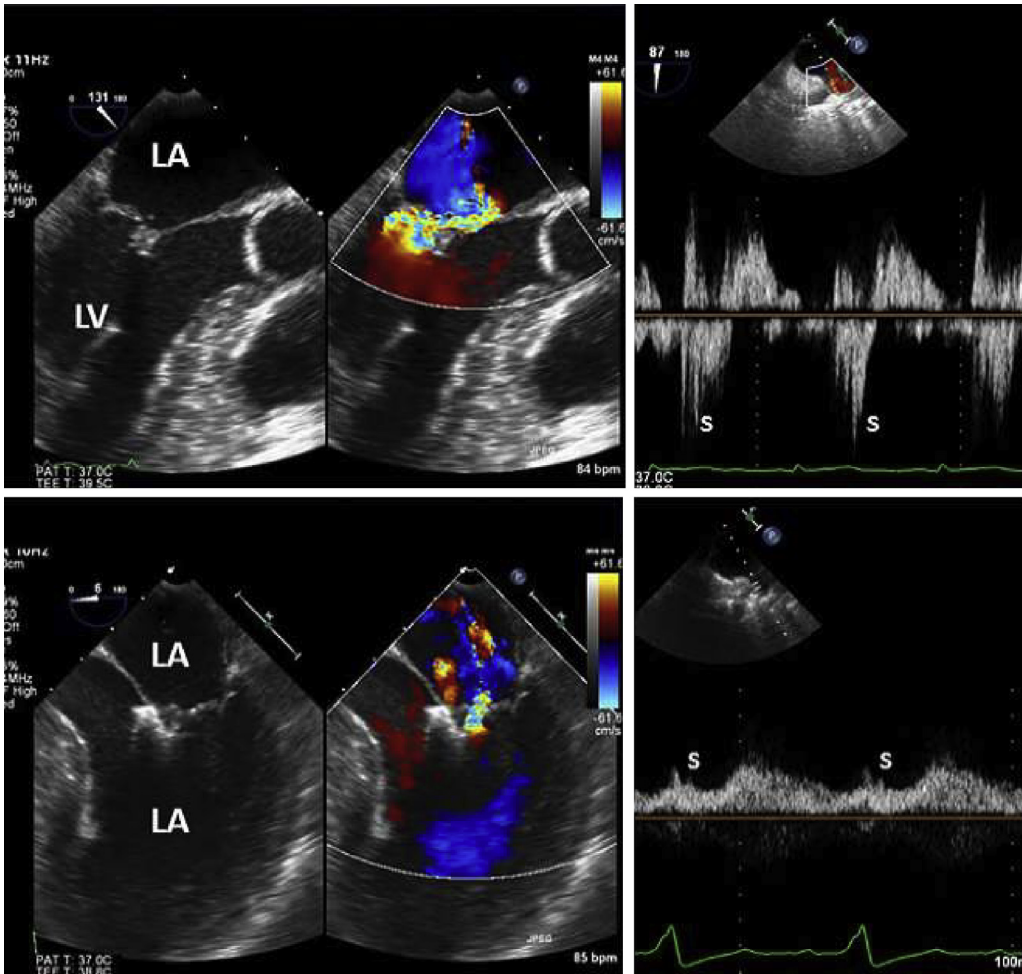


Fig. 21. (Top) Pre-MitraClip and (Bottom) post-MitraClip 2D TEE images showing (top left) severe mitral regurgitation with pulmonary vein systolic flow reversal (top right, S). After MitraClip deployment, the severe MR and flow reversal resolved (bottom left and right, respectively). LA, left atrium; LV, left ventricle.

The 3D TEE in **Fig. 22** illustrates the surgical view of the MV prostheses from an LA aspect. Communication between the echocardiologist and interventionalist is facilitated by referring to the MV prosthesis as a clock face, as seen in **Fig. 22**. In the surgical view, the aorta (at 12-o'clock position, anterior), the IAS, the fossa ovalis (at 3-o'clock position, medial), and the ostium of the LA appendage (at 9-o'clock position, lateral) serve as landmarks. Posterior is defined to be opposite of anterior (6-o'clock position), and the segments in between are defined as anterolateral, anteromedial, posterolateral, and posteromedial. The shape and the extent of the PVML in the anteromedial position can be assessed in detail.

TEE also helps to evaluate contraindications to percutaneous PVML closure. Patients with a

mechanical instability of the prosthetic mitral valve causing a movement of the valve during the cardiac cycle ("rocking valve") (**Fig. 23**), patients in whom the PVML is too large to be percutaneously repaired (the authors do not recommend closing leaks >30% of the valve circumference), or patients with signs of active endocarditis or an intracardiac thrombus should not be considered as candidates for a percutaneous closure procedure. The morphologic evaluation of PV mitral leakages in a posterior location is shown in **Fig. 24**.

Intraprocedural Guidance

To date, there are no guidelines or randomized trials to indicate best practice for PVML closure. Consequently, the technical approach and results

Table 8
Complications that can result from the MitraClip procedure

Complication	Etiology	Treatment/Prevention
Pericardial effusion/tamponade	Transseptal puncture, guidewire or catheter perforation of the LA and LV	Pericardial drainage
Air embolism	Presence of large sheaths that allows air into the venous circulation	Aspiration and flushing of catheter as well as keeping catheter hub lower than the level of heart during catheter insertion or removal
Thrombus formation on the catheter	Presence of foreign objects that predispose to thrombus formation	Maintain ACT of between 250 and 300 s.
Partial Clip detachment	Inappropriate positioning or device malfunction	Appropriate echo guidance, careful assessment of leaflet insertion
Atrial and ventricular arrhythmias	Guidewire or catheter mechanical stimulation	Routine ECG monitoring during the procedure
Entrapment of chordae tendinae by the MitraClip	Inappropriate positioning	Use TEE to carefully monitor catheter and MitraClip position in the LV
Persistent ASD	Iatrogenic due to large size of MitraClip system	Most small and require no treatment; however, if there is SP_{O_2} desaturation due to left-to-right shunting, the defect should be closed at time of the procedure

Abbreviation: ACT, activated clotting time.

of each procedure are case dependent and may even vary for different lesions in the same patient.

During the procedure, continuous hemodynamic and electrocardiographic (ECG) monitoring is important, as wires or catheters that are advanced through a mechanical prosthesis may cause hemodynamic compromise or ventricular tachycardia once introduced into the left ventricle. The procedures are also guided by fluoroscopy (planes that show the valve in orthogonal projections are the most useful for device implantation)

in combination with continuous 2D and 3D TEE monitoring. If available, preacquired computed tomographic angiographic images (4D reconstructions) are displayed in the catheterization laboratory adjacent to the fluoroscopic images to help with probing of the defects and guiding LV puncture when a transapical approach is used.¹⁰⁶ To guide the procedure adequately, knowledge of the different approaches to mitral PVL closure is needed. The different access ways are illustrated in **Fig. 25**.

In most cases, the defect is probed antegradely (see **Fig. 25A**) using a femoral vein access and standard TS puncture techniques to gain entrance into the LA. Alternatively, a TS approach via an internal jugular vein may be preferable in case the leak is located close to the IAS (medial) (see **Fig. 25A**, dashed arrow). The PVML is probed with an end-hole diagnostic right or left Judkins coronary catheter and a hydrophilic 0.035-in wire (occasionally a narrower gauge wire may be helpful). Once across the lesion, a stiffer exchange length guidewire replaces the hydrophilic wire, and a delivery sheath of appropriate size is

Table 9
Recurrence and mortality rates associated with each reoperation for paravalvular leak

Reoperation	Recurrence Rate (%)	Mortality (%)
1st	8	13
2nd	20	15
3rd	42	37

Table 10
Most often used devices for paravalvular mitral leak closure (all used off-label)

Device	Shape of Device	Device Deployment
Amplatzer devices (AGA Medical, MN, USA):		
Septal occluder	Round	Either antegrade or retrograde
Muscular VSD occluder	Round	Either antegrade or retrograde
Duct occluder	Round	Only antegrade
Vascular plugs	Round	Either antegrade or retrograde
Amplatzer vascular plug III (AVP III) occluder	Oval	Either antegrade or retrograde
Vascular coils	Round	Either antegrade or retrograde

Abbreviation: VSD, ventricular septal defect.

advanced into the left ventricle. The proximal disc of the device is opened in the left ventricle; then, the device is pulled back to the ventricular side of the prosthetic valve ring. Once TEE (2D and 3D) and fluoroscopic imaging confirm proper position and orientation of the ventricular aspect of the device, the LA disc is deployed. In cases in which greater stability is needed during the delivery sheath advancement, a circuit is created by snaring the wire in the LA from the LV side via the

femoral artery, thus, creating an arteriovenous loop. The device is then deployed in the way described earlier.

If a retrograde approach is used (see **Fig. 25B**) (eg, in cases in which severe paravalvular regurgitation prevents defect crossing via an antegrade approach), femoral artery access allows a guidewire and support catheter (eg, right coronary Judkins 4.0 or multipurpose catheter) to be advanced across the aortic valve. The PVML is then probed with a long hydrophilic wire. In the next step, the guidewire is snared in the left atrium via TS access and externalized via a femoral vein to provide better support. A delivery sheath is then advanced over the wire through the defect, and the LA disc of the selected device is deployed first. Subsequently, the device is pulled back to the prosthetic valve ring, and if it permits proper device placement and orientation, the LV disc is deployed. With retrograde access, meticulous care is needed not to damage structures located in the left ventricle such as trabeculae, papillary muscles, or chordae. Transapical access (see **Fig. 25C**) is used for defects that cannot be crossed by an antegrade or retrograde approach.¹¹⁴ Ruiz and colleagues¹⁰⁶ described transapical access as being preferable for patients with PVMLs located along the IAS.

The 2D and 3D TEE monitoring of the procedural steps are illustrated in **Fig. 26**.

Postprocedural Assessment

Immediately after device placement, 2D and 3D TEE are used to assess device position, device stability, and interaction with adjacent structures (eg, mechanical valve leaflet obstruction).

A residual leak and the degree of residual regurgitation should be assessed using a multimodal imaging approach according to current

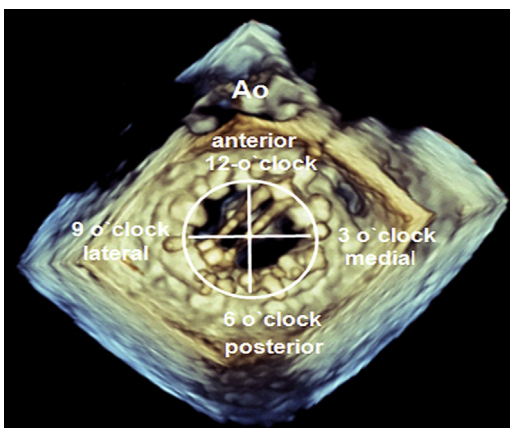


Fig. 22. En face surgical view from the left atrium of a prosthetic mitral valve (RT 3DTEE). The aorta (Ao) is seen at the 12-o'clock position (anterior), at the 3-o'clock position the fossa ovalis (medial) can be seen, the 6-o'clock position is posterior, and the 9-o'clock position (where the left atrial appendage is located) is lateral. The segments in between can be described as anteromedial, anterolateral, posteromedial, and posterolateral. An oval PVML can be seen in the anteromedial position adjacent to the ring of the prosthetic St. Jude Medical valve. ant.lat., anterolateral; ant.med., anteromedial; IAS, intra-atrial septum; post.lat., posterolateral; post.med., posteromedial.

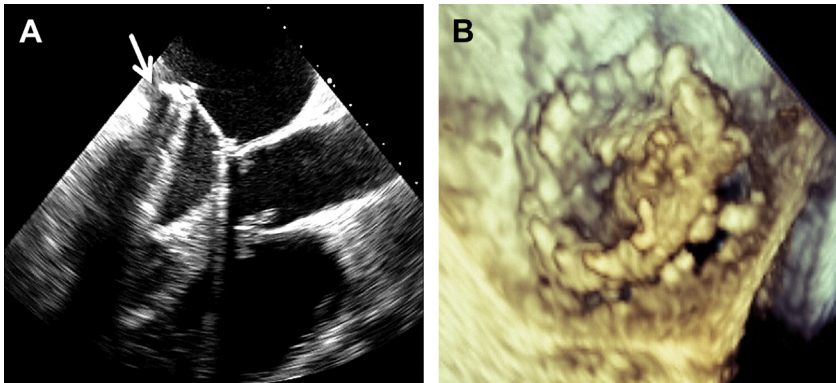


Fig. 23. Example of a nonsuitable patient for PVML closure: (A) A long axis view (100°) reveals a large dehiscence between the mitral annulus and the prosthetic mitral valve (*white arrow*) in the posterior location. (B) The 3D view from the LA confirms a large PVML, nearly half the circumference is ruptured, thus indicating that this is not a candidate for PVML closure.

guidelines.^{10,11,50} Quantification of the paravalvular regurgitation can be achieved by using a volumetric assessment of regurgitation volumes and regurgitant fraction.⁶¹ Complications have to be detected promptly. In **Table 11**, the most frequent

complications occurring during PVML closure, their causes, and their prevention/treatment are summarized.

Postprocedural follow-up studies should include ECG, TTE, TEE, and assessment for hemolysis.

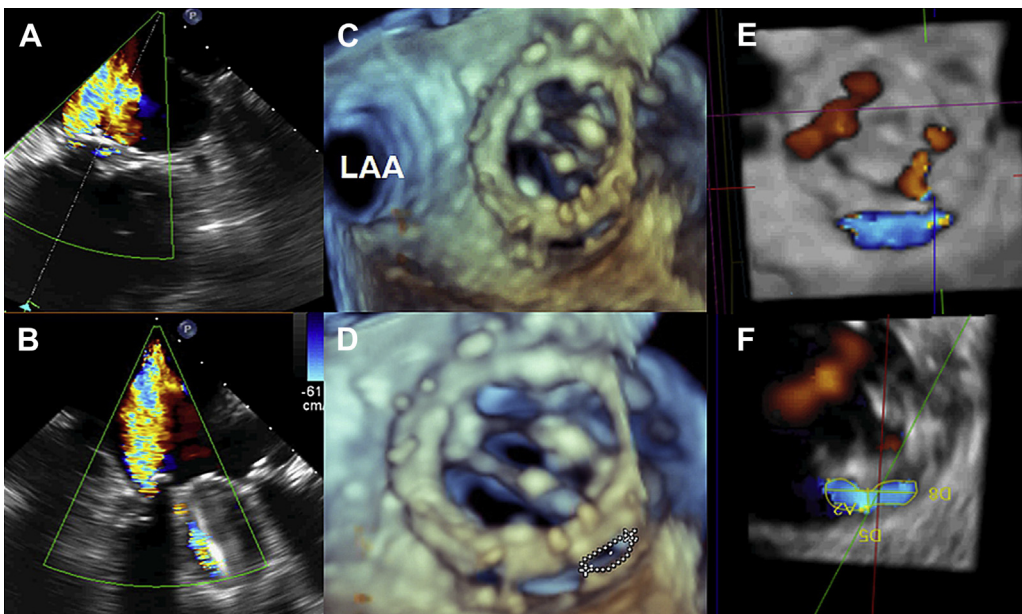


Fig. 24. Evaluation of a patient after implantation of a mechanical SJM valve with 3 paravalvular leaks in posterior location with 2D TEE and 3D TEE modalities (Philips iE33 including QLAB analysis). In (A), an intercommissural 2D TEE view (65°) is shown, and in (B), the corresponding long axis x-plane view (155°) showing a color flow jet posteriorly next to the prosthetic valve ring. In (C), the posterior leaks are presented in an en face view from the LA side, thus allowing a more detailed analysis and clarifying that 3 leaks separated by small tissue bridges are present; in (D), the direct delineation of one of the defects in an RT 3D TEE still frame image is shown. A full volume acquisition with color Doppler demonstrates the extension of the color jet adjacent to the prosthetic ring in (E), and in (F) the QLAB analysis of the regurgitant area is seen. LA, left atrium; LAA, left atrial appendage.

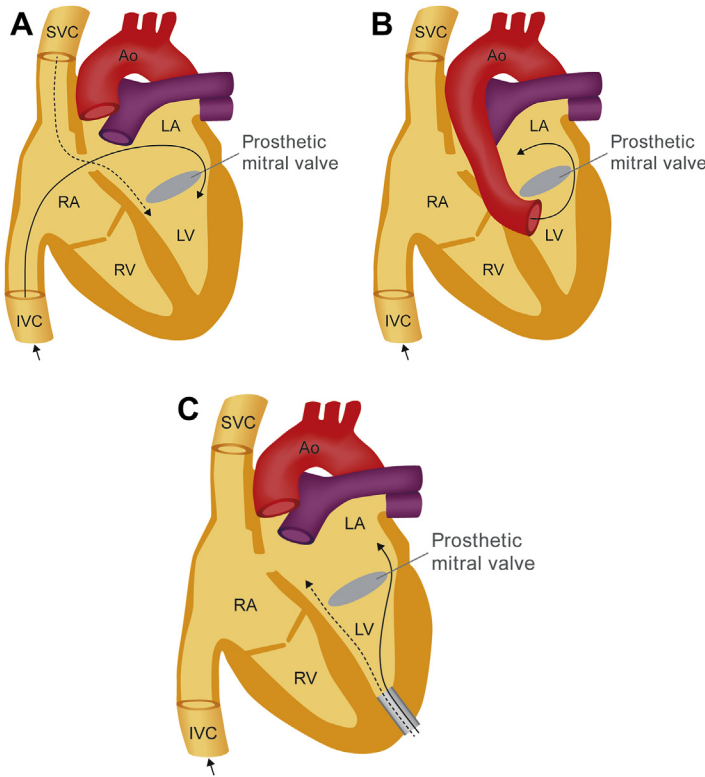


Fig. 25. Different approaches to PVML closure. (A) Antegrade approach via a transseptal access either from the femoral vein (black arrow) or from the jugular vein (dashed black arrow). (B) Retrograde access via a femoral artery and the aorta into the LV and through the PVML into the LA (the wire can be snared in the LA to create an arteriovenous loop). (C) Transapical access. Ao, aorta; IVC, inferior vena cava; LA, left atrium; LV, left ventricle; RA, right atrium; RV, right ventricle; SVC, superior vena cava.

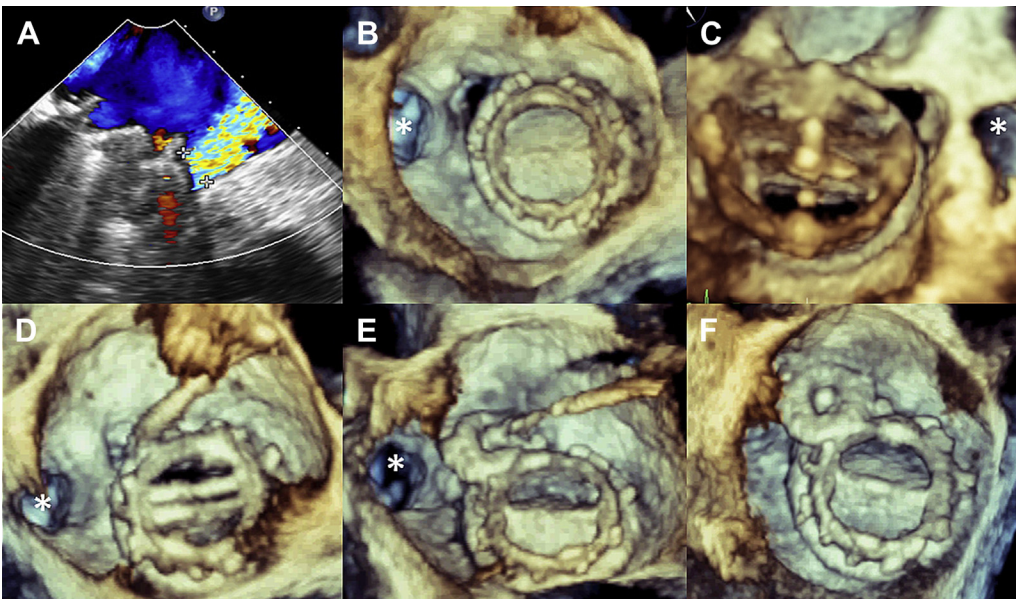


Fig. 26. Monitoring of a paravalvular leak closure in anterolateral position with a muscular ventricular septal defect occluder using an antegrade approach (the entrance of the LAA is marked with a white star). (A) 2D TEE (125°): The measurement of the width of the color jet through the defect is shown; (B) left atrial aspect of the defect in an en face view; (C) left ventricular aspect of the defect in an en face view; (D) the delivery catheter is advanced antegradely through the defect (LA aspect); (E) (LA aspect) both occluder discs are deliberated, and the LA disc can be identified. The device is still attached to the delivery cable (F) left atrial en face view showing the final device position. LA, left atrium; LAA, left atrial appendage.

Table 11
Complications that can occur from paravalvular mitral leak closure

Complication	Etiology	Treatment/Prevention
Pericardial effusion/ tamponade	Transseptal puncture, guidewire or catheter perforation of LA and LV	Pericardial drainage, surgery if needed
Air embolism	Presence of large sheaths that allow air into the circulation	Aspiration and flushing of catheter as well as keeping catheter hub lower than the level of heart during catheter insertion or removal
Thrombus formation either intracardiac or attached to wires/catheters	Presence of foreign material, which predispose to thrombus formation	Maintain ACT of between 250 and 300 s
Failure to cross the leak with the delivery sheath	Severe friction	Usage of hydrophilic sheaths, change of wire
Difficulty to probe the lesions	Difficult 3-dimensional navigation in large cardiac chambers	Usage of a steerable (eg, Agilis, St. Jude Medical) sheath that can be orientated toward the defect under real-time 3D TEE imaging guidance
Atrial and ventricular arrhythmias	Guidewire or catheter mechanical stimulation	Routine ECG monitoring during the procedure
Interference with valve leaflets	Deployed occluder constrains the valve mechanically	Appropriate echo guidance; repositioning of the device leads occasionally to satisfactory results; if this is not the case, surgery should be considered
Wire entrapment	Inappropriate positioning	Use TEE to carefully monitor catheter and wire position
Persistent residual leak	Due to mismatch of the device and defect shapes, additional leaks or delayed or even absent endothelialization ¹¹⁵	An additional PVML closure procedure may be considered, alternatively surgery
Mitral leaflet erosion	Described by frame fractures of the device ¹¹⁶	Surgical repair
Device-related infection	Any implanted foreign body is associated with the risk of device-related infection	Prevention: periinterventional administration of antibiotics If an infection occurs, in most cases the surgical device removal and valvular replacement or repair is necessary
Hemolysis	Occurs most likely shortly after the procedure (multiple and smaller wholes are more frequently associated with hemolysis)	Blood transfusion if necessary, monitoring; with ongoing endothelialization hemolysis may decrease over time. If it persists, a second closure procedure or surgical repair should be considered
Persistent ASD	Iatrogenic due to transseptal sheath	Most remain small and require no treatment
Device embolization	Unsecure position of the device due to a mismatch of the device size and the defect	Snare with large loop diameters (25–40 mm) should be close at hand to capture and retrieve the occluder (eg, Amplatz Goose Neck, eV3, MN, USA, or Lassos, Dr. Osypka, Germany). Rarely surgical removal may be necessary

Abbreviation: ACT, activated clotting time.

SUMMARY

As the mitral leaflets cannot be assessed by fluoroscopy, preprocedural assessment, procedural guidance, and postprocedural assessment of percutaneous mitral interventions for MS, MR, and MV PVLs rely heavily on echocardiography. Although 2D TEE has played a major role in guidance of the procedures, 3D TEE provides more detailed information on the MV anatomy and catheter and device position. Thus, combining 2D and 3D TEE improves results and reduces procedure time. Consequently, there is an increasing reliance on 3D TEE for mitral interventions.^{57,117} A newly developed EchoNavigator system (Philips Healthcare, Andover, MA) may further facilitate procedural guidance by matching echocardiographic and fluoroscopic images. The EchoNavigator system is based upon technology that automatically recognizes and tracks the position of the TEE probe. Although only limited clinical data are available at this time, these new features of the EchoNavigator system may facilitate guidance of the procedure by supporting the understanding of the spatial relation between the echo and x-ray image, thus making the interpretation and understanding of anatomic structures rendered by TEE easier. Echocardiography during percutaneous mitral valve procedures has evolved from transthoracic 2D echo guidance of PBMV to more complex procedures such as MitraClip and repair of PVLs. Imaging technology is continuing to evolve and improve. At present, 3D TEE and fluoroscopy are essential for the optimal guidance and outcomes of transcatheter MV procedures.

REFERENCES

1. Iung B, Cormier B, Ducimetiere P, et al. Immediate results of percutaneous mitral commissurotomy. A predictive model on a series of 1514 patients. *Circulation* 1996;94:2124–30.
2. Palacios IF. Farewell to surgical mitral commissurotomy for many patients. *Circulation* 1998;97:223–6.
3. Hung JS, Chern MS, Wu JJ, et al. Short and long-term results of catheter balloon percutaneous transvenous mitral commissurotomy. *Am J Cardiol* 1991;67:854–62.
4. Dean LS, Mickel M, Bonan R, et al. Four-year follow-up of patients undergoing percutaneous balloon mitral commissurotomy: a report from the National Heart, Lung, and Blood Institute Balloon Valvuloplasty Registry. *J Am Coll Cardiol* 1996;28:1452–7.
5. Abascal VM, Wilkins GT, Choong CY, et al. Echocardiographic evaluation of mitral valve structure and function in patients followed for at least 6 months after percutaneous balloon mitral valvuloplasty. *J Am Coll Cardiol* 1988;12:606–15.
6. Post JR, Feldman T, Isner J, et al. Inoue balloon mitral valvotomy in patients with severe valvular and subvalvular deformity. *J Am Coll Cardiol* 1995;25:1129–36.
7. Hernandez R, Banuelos C, Alfonso F, et al. Long-term clinical and echocardiographic follow-up after percutaneous mitral valvuloplasty with the Inoue balloon. *Circulation* 1999;99:1580–6.
8. Iung BL, Garbarz E, Michaud P, et al. Late results of percutaneous mitral commissurotomy in a series of 1024 patients: analysis of late clinical deterioration: frequency, anatomic findings and predictive factors. *Circulation* 1999;99:3272–8.
9. Chen CR, Cheng TO, Chen JY, et al. Long-term results of percutaneous balloon mitral valvuloplasty for mitral stenosis: a follow-up study to 11 years in 202 patients. *Cathet Cardiovasc Diagn* 1998;43:132–9.
10. Borger MA, Carrel TP, DeBonis M, et al. Guidelines on the management of valvular heart disease (version 2012) the Joint Task Force on the Management of Valvular Heart Disease of the European Society of Cardiology (ESC) and the European Association for Cardio-Thoracic Surgery (EACTS). *Eur Heart J* 2012;33:2451–96. <http://dx.doi.org/10.1093/eurheartj/ehs109>.
11. Bonow RO, Carabello BA, Chatterjee K, et al. American College of Cardiology/American Heart Association Task Force on Practice Guidelines. 2008 focused update incorporated into the ACC/AHA 2006 guidelines for the management of patients with valvular heart disease: a report of the American College of Cardiology/American Heart Association Task Force on Practice Guidelines/Writing Committee to revise the 1998 guidelines for the management of patients with valvular heart disease). Endorsed by the Society of Cardiovascular Anesthesiologists, Society for Cardiovascular Angiography and Interventions and Society of Thoracic Surgeons. *J Am Coll Cardiol* 2008;52(13):e1–142.
12. Vahanian A, Baumgartner H, Bax J, et al. Guidelines on the management of valvular heart disease of the European Society of Cardiology. *Eur Heart J* 2007;28:230–68.
13. Wood P. An appreciation of mitral stenosis. I: Clinical features. *Br Med J* 1954;4870:1051.
14. Rowe JC, Bland EF, Sprague HB, et al. The course of mitral stenosis without surgery: ten- and twenty-year perspectives. *Ann Intern Med* 1960;52:741–9.
15. Baumgartner H, Hung J, Bermejo J, et al. Echocardiographic assessment of valve stenosis: EAE/ASE recommendations for clinical practice. *J Am Soc Echocardiogr* 2009;22(1):1–23.
16. Faletra F, Pezzano A Jr, Fusco R, et al. Measurement of mitral valve area in mitral stenosis: four

- echocardiographic measurements compared with direct measurements of anatomic orifices. *J Am Coll Cardiol* 1996;28:1190–7.
17. Min SY, Song JM, Kim YJ, et al. Discrepancy between mitral valve areas measured by two-dimensional planimetry and three dimensional transesophageal echocardiography in patients with mitral stenosis. *Heart* 2013;99(4):253–8.
 18. Schlosshan D, Aggarwal G, Mathur G, et al. Real-time 3D transesophageal echocardiography for the evaluation of rheumatic mitral valve stenosis. *J Am Coll Cardiol* 2011;4(6):580–8.
 19. Sugeng L, Weinert L, Lammertin G, et al. Accuracy of mitral valve area measurements using transthoracic rapid freehand 3-dimensional scanning: comparison with noninvasive and invasive measurements. *J Am Soc Echocardiogr* 2003;16(12):1292–300.
 20. Thomas JD, Newell JB, Choong CY, et al. Physical and physiological determinants of transmitral velocity: numerical analysis. *Am J Physiol* 1991;260(5 Pt 2):H1718–31.
 21. Nishimura RA, Rihal CS, Tajik AJ, et al. Accurate measurement of the transmitral gradient in patients with mitral stenosis: a simultaneous catheterization and Doppler echocardiographic study. *J Am Coll Cardiol* 1994;24:152–8.
 22. Gorlin R, Gorlin SG. Hydraulic formula for calculation of the area of the stenotic mitral valve, other cardiac valves, and central circulatory shunts. *Am Heart J* 1951;41:1–29.
 23. Wilkins GT, Weyman AE, Abascal VM, et al. Percutaneous balloon dilatation of the mitral valve: an analysis of echocardiographic variables related to outcome and the mechanism of dilatation. *Br Heart J* 1988;60:299–308.
 24. Chen CG, Wang X, Wang Y, et al. Value of two-dimensional echocardiography in selecting patients and balloon sizes for percutaneous balloon mitral valvuloplasty. *J Am Coll Cardiol* 1989;14(7):1651–8.
 25. Reid CL, Chandraratna PA, Kawanishi DT, et al. Influence of mitral valve morphology on double-balloon catheter balloon valvuloplasty in patients with mitral stenosis. Analysis of factors predicting immediate and 3-month results. *Circulation* 1989;80(3):515–24.
 26. Nobuyoshi M, Hamasaki N, Kimura T, et al. Indications, complications, and short-term clinical outcome of percutaneous transvenous mitral commissurotomy. *Circulation* 1989;80(4):782–92.
 27. Cannan CR, Nishimura RA, Reeder GS, et al. Echocardiographic assessment of commissural calcium: a simple predictor of outcome after percutaneous mitral balloon valvotomy. *J Am Coll Cardiol* 1997;29:175–80.
 28. Sutaria N, Northridge DB, Shaw TR. Significance of commissural calcification on outcome of mitral balloon valvotomy. *Heart* 2000;84:398–402.
 29. Padiyal LR, Freitas N, Sagie A, et al. Echocardiography can predict which patients will develop severe mitral regurgitation after percutaneous mitral valvotomy. *J Am Coll Cardiol* 1996;27:1225–31.
 30. Lung B, Cormier B, Ducimetiere P, et al. Functional results 5 years after successful percutaneous mitral commissurotomy in a series of 528 patients and analysis of predictive factors. *J Am Coll Cardiol* 1996;27:407–14.
 31. Anwar AM, Attia WM, Nosir YF, et al. Validation of a new score for the assessment of mitral stenosis using real-time three-dimensional echocardiography. *J Am Soc Echocardiogr* 2010;23(1):13–22.
 32. Palacios IF, Sanchez PL, Harrell LC, et al. Which patients benefit from percutaneous mitral balloon valvuloplasty? Prevalvuloplasty and postvalvuloplasty variables that predict long term outcome. *Circulation* 2002;105:1465–71.
 33. Chen CR, Cheng TO. Percutaneous balloon mitral valvuloplasty by the Inoue technique: a multicenter study of 4832 patients in China. *Am Heart J* 1995;129:1197–203.
 34. Thomas JD, Wilkins GT, Choong CY, et al. Inaccuracy of mitral pressure half-time immediately after percutaneous mitral valvotomy. Dependence on transmitral gradient and left atrial and ventricular compliance. *Circulation* 1988;78:980–93.
 35. Otto CM, Davis KB, Holmes DR, et al. Methodologic issues in clinical evaluation of stenosis severity in adults undergoing aortic or mitral balloon valvuloplasty. *Am J Cardiol* 1992;69:1607–16.
 36. Reid CL, Rahimtoola SH. The role of echocardiography/Doppler in catheter balloon treatment of adults with aortic and mitral stenosis. *Circulation* 1991;84:240–9.
 37. Vahanian A, Michel PL, Cormier B, et al. Results of percutaneous mitral commissurotomy in 200 patients. *Am J Cardiol* 1989;63:847–52.
 38. Zamorano J, Perez de Isal L, Sugeng L, et al. Non-invasive assessment of mitral valve area during percutaneous balloon mitral valvuloplasty: role of real-time 3D echocardiography. *Eur Heart J* 2004;25:2086–91.
 39. Messika-Zeitoun D, Blanc J, Lung B, et al. Impact of degree of commissural opening after percutaneous mitral commissurotomy on long-term outcome. *JACC Cardiovasc Imaging* 2009;2:1–7.
 40. Pan M, Medina A, Suarez de Lezo J, et al. Factors determining late success after mitral balloon valvulotomy. *Am J Cardiol* 1993;71(13):1181–5.
 41. Zhang HP, Yen GS, Allen JW, et al. Comparison of late results of balloon valvotomy in mitral stenosis with versus without mitral regurgitation. *Am J Cardiol* 1998;81:51–5.
 42. Jorge E, Baptista R, Faria H, et al. Mean pulmonary arterial pressure after percutaneous mitral

- valvuloplasty predicts long-term adverse outcomes. *Rev Port Cardiol* 2012;31(1):19–25.
43. Jneid H, Cruz-Gonzalez I, Sanchez-Ledesma M, et al. Impact of pre- and postprocedural mitral regurgitation on outcomes after percutaneous mitral valvuloplasty for mitral stenosis. *Am J Cardiol* 2009;104(8):1122–7.
 44. Conte J, Weissman N, Dearani JA, et al. A North American, prospective, multicenter assessment of the Mitroflow aortic pericardial prosthesis. *Ann Thorac Surg* 2010;90(1):144–152.e1–3.
 45. Alfieri O, Maisano F, DeBonis M, et al. The edge-to-edge technique in mitral valve repair: a simple solution for complex problems. *J Thorac Cardiovasc Surg* 2001;122:674–81.
 46. Feldman T, Wasserman HS, Herrmann HC, et al. Percutaneous mitral valve repair using the edge-to-edge technique. Six-month results of the EVEREST Phase I Clinical Trial. *J Am Coll Cardiol* 2005;46(11):2134–40.
 47. Feldman T, Kar S, Rinaldi M, et al, EVEREST Investigators. Percutaneous mitral repair with the MitraClip system: safety and midterm durability in the initial EVEREST (Endovascular Valve Edge-to-Edge Repair Study) cohort. *J Am Coll Cardiol* 2009;54(8):686–94.
 48. Franzen O, Baldus S, Rudolph V, et al. Acute outcomes of MitraClip therapy for mitral regurgitation in high-surgical-risk patients: emphasis on adverse valve morphology and severe left ventricular dysfunction. *Eur Heart J* 2010;31:1373–81.
 49. Feldman T, Foster E, Glower DD, et al, EVEREST II Investigators. Percutaneous repair or surgery for mitral regurgitation. *N Engl J Med* 2011;364(15):1395–406.
 50. Lancelotti P, Moura L, Pierard LA, et al. European Association of Echocardiography recommendations for the assessment of valvular regurgitation. Part 2: mitral and tricuspid regurgitation (native valve disease). *Eur J Echocardiogr* 2010;11:307–32.
 51. Nguyen C, Lee E, Luo H, et al. Echocardiographic guidance for diagnostic and therapeutic procedures. *Cardiovasc Diag Ther* 2011;1:11–36.
 52. La Canna G, Arendar I, Maisano F, et al. Real-time three-dimensional transesophageal echocardiography for assessment of mitral valve functional anatomy in patients with prolapse-related regurgitation. *Am J Cardiol* 2011;107(9):1365–74.
 53. Grewal J, Mankad S, Freeman WK, et al. Real-time three-dimensional transesophageal echocardiography in the intraoperative assessment of mitral valve disease. *J Am Soc Echocardiogr* 2009;22(1):34–41.
 54. Ben Zekry S, Nagueh SF, Little SH, et al. Comparative accuracy of two- and three-dimensional trans-thoracic and transesophageal echocardiography in identifying mitral valve pathology in patients undergoing mitral valve repair: initial observations. *J Am Soc Echocardiogr* 2011;24(10):1079–85.
 55. Thompson KA, Shiota T, Tolstrup K, et al. Utility of three-dimensional transesophageal echocardiography in the diagnosis of valvular perforations. *Am J Cardiol* 2011;107(1):100–2.
 56. Salcedo EE, Quaipe RA, Seres T, et al. A framework for systematic characterization of the mitral valve by real-time three-dimensional transesophageal echocardiography. *J Am Soc Echocardiogr* 2009;22(10):1087–99.
 57. Lang RM, Badano LP, Tsang W, et al. EAE/ASE recommendations for image acquisition and display using three-dimensional echocardiography. *J Am Soc Echocardiogr* 2012;25:3–46.
 58. Biner S, Perk G, Kar S, et al. Utility of combined two-dimensional and three-dimensional transesophageal imaging for catheter-based mitral valve clip repair of mitral regurgitation. *J Am Soc Echocardiogr* 2011;24(6):611–7.
 59. Slipczuk L, Siegel RJ, Jilaihawi H, et al. Optimizing procedural outcome in percutaneous mitral valve therapy using transesophageal imaging: a stepwise analysis. *Expert Rev Cardiovasc Ther* 2012;10:901–6.
 60. Lin BA, Forouhar AS, Pahlevan NM, et al. Color Doppler jet area overestimates regurgitant volume when multiple jets are present. *J Am Soc Echocardiogr* 2010;23(9):993–1000.
 61. Blumlein S, Bouchard A, Schiller NB, et al. Quantitation of mitral regurgitation by Doppler echocardiography. *Circulation* 1986;74:306–14.
 62. Kahlert P, Pflicht B, Schenk IM, et al. Direct measurement of size and shape of non-circular vena contracta in functional versus organic mitral regurgitation using real time 3-dimensional echocardiography. *J Am Soc Echocardiogr* 2008;21:912–21.
 63. Chaim Y, Hung J, Chua S, et al. Direct measurement of vena contracta area by real-time 3-dimensional echocardiography for assessing severity of mitral regurgitation. *Am J Cardiol* 2009;104:978–83.
 64. Herrmann HC, Rohatgi S, Wasserman HS, et al. Mitral valve hemodynamic effects of percutaneous edge-to-edge repair with the MitraClip™ device for mitral regurgitation. *Catheter Cardiovasc Interv* 2006;68:821–8.
 65. Herrmann HC, Kar S, Siegel R, et al. Effect of percutaneous mitral repair with the MitraClip device on mitral valve area and gradient. *EuroIntervention* 2008;4:437–42.
 66. Bernal J, Rabasa J, Gutierrez-Garcia F, et al. The CarboMedics valve: experience with 1,049 implants. *Ann Thorac Surg* 1998;65:137–43.
 67. Orzulak TA, Schaff HV, Danielson GK, et al. Results of reoperation for periprosthetic leakage. *Ann Thorac Surg* 1983;35:584–9.

68. Nakano K, Koyanagi H, Hashimoto A, et al. Twelve years experience with St. Jude Medical prosthesis. *Ann Thorac Surg* 1994;57:697–703.
69. Arom KV, Nicoloff DM, Kersten TE, et al. Ten years experience with St. Jude Medical valve prosthesis. *Ann Thorac Surg* 1989;47:831–7.
70. Rutledge R, Kim J, Appelbaum R. Actuarial analysis of prosthetic valve endocarditis in 1,598 patients with mechanical and bioprosthetic valves. *Arch Surg* 1985;120:469–72.
71. Ivert TS, Dismukes WE, Cobbs CG. Prosthetic valve endocarditis. *Circulation* 1984;69:223–32.
72. Arvay A, Lengyel M. Incidence and risk factors of prosthetic valve endocarditis. *Eur J Cardiothorac Surg* 1988;2:340–6.
73. Lehmann S, Walther T, Leontyev S, et al. Eight-year follow-up after prospectively randomized implantation of different mechanical aortic valves. *Clin Res Cardiol* 2008;97(6):376–82.
74. Englberger L, Schaff HV, Jamieson WR, et al. Importance of implant technique on risk of major paravalvular leak (PVL) after St. Jude mechanical heart valve replacement: a report from the Artificial Valve Endocarditis Reduction Trial (AVERT). *Eur J Cardiothorac Surg* 2005;28(6):838–43.
75. Emery RW, Krogh CC, Arom KV, et al. The St. Jude Medical cardiac valve prosthesis: a 25-year experience with single valve replacement. *Ann Thorac Surg* 2005;79(3):776–82 [discussion: 782–3].
76. Nitter-Hauge S, Abdelnoor M. Ten-year experience with the Medtronic Hall valvular prosthesis. A study of 1,104 patients. *Circulation* 1989;80(3 Pt 1):143–8.
77. Li HH, Hahn J, Urbanski P, et al. Intermediate-term results with 1,019 CarboMedics aortic valves. *Ann Thorac Surg* 2001;71(4):1181–7 [discussion: 1187–8].
78. Spiliopoulos K, Haschemi A, Parasiris P, et al. Sorin Bicarbon bileaflet valve: a 9.8-year experience. Clinical performance of the prosthesis after heart valve replacement in 587 patients. *Interact Cardiovasc Thorac Surg* 2009;8(2):252–9.
79. Al-Khaja N, Belboul A, Larsson S, et al. Eleven years' experience with Carpentier-Edwards biological valves in relation to survival and complications. *Eur J Cardiothorac Surg* 1989;3(4):305–11.
80. Folliguet TA, Dibie A, Czitrom D, et al. Ten-years' clinical experience with the Sorin Pericarbon valve. *J Heart Valve Dis* 2000;9(3):423–8.
81. Riess FC, Cramer E, Hansen L, et al. Clinical results of the Medtronic Mosaic porcine bioprosthesis up to 13 years. *Eur J Cardiothorac Surg* 2010;37(1):145–53.
82. Bottio T, Rizzoli G, Thiene G, et al. Hemodynamic and clinical outcomes with the Biocor valve in the aortic position: an 8-year experience. *J Thorac Cardiovasc Surg* 2004;127(6):1616–23.
83. Ionescu A, Fraser AG, Butchart EG. Prevalence and clinical significance of incidental paraprosthetic valvar regurgitation: a prospective study using transesophageal echocardiography. *Heart* 2003;89:1316–21.
84. Duvernoy WF, Gonzalez-Lavin L, Anbe DT. Spontaneous closure of paravalvular leak after mitral valve replacement. *Chest* 1975;68:102–4.
85. Pate GE, Zubaidi A, Chandavimol M, et al. Percutaneous closure of prosthetic paravalvular leaks: case series and review. *Catheter Cardiovasc Interv* 2006;68:528–33.
86. Rallidis LS, Moysakakis IE, Ikonomidis I, et al. Natural history of early aortic paraprosthetic regurgitation: a five-year follow-up. *Am Heart J* 1999;138:351–7.
87. Miller DL, Morris JJ, Schaff HV, et al. Reoperation for aortic valve periprosthetic leakage: identification of patients at risk and results of operation. *J Heart Valve Dis* 1995;4:160–5.
88. Jindani A, Neville EM, Venn G, et al. Paraprosthetic leak: a complication of cardiac valve replacement. *J Cardiovasc Surg (Torino)* 1991;32:503–8.
89. Safi AM, Kwan T, Afflu E, et al. Paravalvular regurgitation: a rare complication following valve replacement surgery. *Angiology* 2000;51:479–87.
90. Genoni M, Franzen D, Tavakoli R, et al. Does the morphology of mitral paravalvular leaks influence symptoms and hemolysis? *J Heart Valve Dis* 2001;10(4):426–30.
91. Pate G, Webb J, Thompson C, et al. Percutaneous closure of a complex prosthetic mitral paravalvular leak using transesophageal echocardiographic guidance. *Can J Cardiol* 2004;20:452–5.
92. Chen YT, Kan MN, Chen JS, et al. Detection of prosthetic mitral valve leak: a comparative study using transesophageal echocardiography, transthoracic echocardiography and auscultation. *J Clin Ultrasound* 1990;18:557–61.
93. Sinha DP, Biswas S, Kumar S, et al. Studies on prosthetic valve function. A transesophageal echocardiographic assessment. *J Assoc Physicians India* 1996;44:525–8.
94. Faletta F, De Chiara F, Corno R, et al. Additional diagnostic value of multiplane echocardiography over biplane imaging in assessment of mitral prosthetic valves. *Heart* 1996;75:609–13.
95. Echevarria JR, Bernal JM, Rabasa JM, et al. Reoperation for bioprosthetic valve dysfunction. A decade of clinical experience. *Eur J Cardiothorac Surg* 1991;5:523–6 [discussion: 527].
96. Expósito V, Garcia-Camarero T, Bernal JM, et al. Repeat mitral valve replacement: 30-years experience. *Rev Esp Cardiol* 2009;62(8):929–32.
97. Hourihan M, Perry SB, Mandell VS, et al. Transcatheter umbrella closure of valvular and paravalvular leaks. *J Am Coll Cardiol* 1992;20(6):1371–7.
98. Hein R, Wunderlich N, Robertson G, et al. Catheter closure of paravalvular leak. *EuroIntervention* 2006;3:318–25.

99. Del Valle-Fernandez R, Martinez C, Jelmin V, et al. Paravalvular leak closure: single-center experience. *Eur Heart J* 2009;30(Abtract Suppl):920.
100. Pate GE, Thomson CR, Munt BI, et al. Techniques for percutaneous closure of prosthetic paravalvular leaks. *Catheter Cardiovasc Interv* 2006;67:158–66.
101. Shapira Y, Hirsch R, Kornowski R, et al. Percutaneous closure of perivalvular leaks with Amplatzer occluders: feasibility, safety, and short term results. *J Heart Valve Dis* 2007;16:305–13.
102. Sorajja P, Cabalka AK, Hagler DJ, et al. Successful percutaneous repair of perivalvular prosthetic regurgitation. *Catheter Cardiovasc Interv* 2007;70:815–23.
103. Cortes M, Garcia E, Garcia-Fernandez MA, et al. Usefulness of transesophageal echocardiography in percutaneous transcatheter repair of paravalvular mitral regurgitation. *Am J Cardiol* 2008;101:382–6.
104. Garcia Borbolla Fernandez R, Sanch Jaldon M, Calle Perez G, et al. Percutaneous treatment of mitral valve periprosthetic leakage. An alternative to high-risk surgery? *Rev Esp Cardiol* 2009;62:438–41.
105. Nietlispach F, Johnson M, Moss RR, et al. Transcatheter closure of paravalvular defects using a purpose specific occluder. *JACC Cardiovasc Interv* 2010;3:759–65.
106. Ruiz C, Jelmin V, Kronzon I, et al. Clinical outcomes in patients undergoing percutaneous closure of periprosthetic paravalvular leaks. *J Am Coll Cardiol* 2011;58:2210–7.
107. Foster GP, Isselbacher EM, Rose GA, et al. Accurate localization of mitral regurgitant defects using multiplane transesophageal echocardiography. *Ann Thorac Surg* 1998;65(4):1025–31.
108. Chambers J, Monaghan M, Jackson G. Colour flow Doppler mapping in the assessment of prosthetic valve regurgitation. *Br Heart J* 1989;62:1–8.
109. Kapur KK, Fan P, Nanda NC, et al. Doppler color flow mapping in the evaluation of prosthetic mitral and aortic valve function. *J Am Coll Cardiol* 1989;13:1561–71.
110. Vitarelli A, Conde Y, Cimino E, et al. Assessment of severity of mechanical prosthetic mitral regurgitation by transesophageal echocardiography. *Heart* 2004;90:539–44.
111. Kronzon I, Sugeng L, Perk G, et al. Real-time 3-dimensional transesophageal echocardiography in the evaluation of post-operative mitral annuloplasty ring and prosthetic valve dehiscence. *J Am Coll Cardiol* 2009;53:1543–7.
112. Garcia-Fernandez MA, Cortes M, Garcia-Robles JA, et al. Utility of real-time three-dimensional echocardiography in evaluating the success of percutaneous transcatheter closure of mitral paravalvular leaks. *J Am Soc Echocardiogr* 2010;23:26–32.
113. Biner S, Kar S, Siegel RJ, et al. Value of colour Doppler three-dimensional transesophageal echocardiography in the percutaneous closure of mitral prosthesis paravalvular leak. *Am J Cardiol* 2010;105:984–9.
114. Swaans MJ, Post MC, van der Ven J, et al. Transapical treatment of paravalvular leaks in patients with a logistic EuroSCORE of more than 15%: acute and 3-months outcomes of a “proof of concept” study. *Catheter Cardiovasc Interv* 2012;79:741–7.
115. Özkan M, Astargioglu MA, Gürsoy O. Evaluation of endothelialisation after percutaneous closure of paravalvular leaks. *J Invasive Cardiol* 2012;24(4):E72–4.
116. Rogers JH, Morris AS, Takeda PA, et al. Bioprosthetic leaflet erosion after percutaneous mitral paravalvular leak closure. *J Am Coll Cardiol* 2010;3(1):122–3.
117. Wunderlich N, Franke J, Wilson N, et al. 3D echoguidance for structural heart interventions. *Intervent Cardiol* 2009;4(1):16–20.

APPENDIX A: ASSESSMENT OF MS SEVERITY

The MV area can be also be derived from Doppler echocardiography using the diastolic pressure half-time ($T_{1/2}$) method. $T_{1/2}$ is obtained by tracing the deceleration slope of the E-wave on Doppler spectral display of transmitral inflow. The MV area can be calculated from the following formula: $220/(T_{1/2})$. Limitations of this method include abnormal LA or LV compliance, associated aortic regurgitation, ASD, and patients who have previously had mitral valvuloplasty.

In case additional measurements are needed, the continuity equation and PISA methods can be used. The calculation of the MVA using the continuity equation is based on the assumption that the filling volume of diastolic mitral flow is equal to aortic stroke volume. The following formula is used:

$$MVA = \pi \left(\frac{D^2}{4} \right) \left(\frac{VTI \text{ Aorta (cm)}}{VTI \text{ mitral (cm)}} \right)$$

D = LVOT diameter

The accuracy and reproducibility of the method are limited in that the number of measurements needed for this calculation increases the probability that measurement errors occur. In case atrial fibrillation or relevant mitral or aortic regurgitation is present, the continuity equation cannot be used.

The PISA method permits the assessment of mitral flow based on the hemispheric shape of the convergence zone of mitral flow in diastole on the LA side as seen by color Doppler. Subsequently, the MVA is calculated by dividing

mitral volume flow by the maximum velocity of mitral flow in diastole as assessed by color CW Doppler:

$$\text{MVA} = \pi (r^2) (V_{\text{alias}}) / \text{Peak } V_{\text{mitral}} \times \alpha / 180^\circ$$

r = radius of the hemispheric convergence zone (cm)

V_{alias} = aliasing velocity (cm/s)

Peak V_{mitral} = peak velocity of mitral inflow assessed with CW Doppler (cm/s)

α = opening angle of mitral leaflets relative to flow direction

This method is technically demanding but can be used in the presence of relevant MR.